AD-A039 661 HUGHES RESEARCH LABS MALIBU CALIF F/G 17/2
SYSTEMATIC SURVEY OF NAVAL SURVEILLANCE AND COMMUNICATION SYSTE--ETC(U)
MAR 77 P SCHWARTZ, L ROTH N00173-76-C-0389
UNCLASSIFIED NL

| OF |
AD
A039661

END

DATE
FILMED
6-77

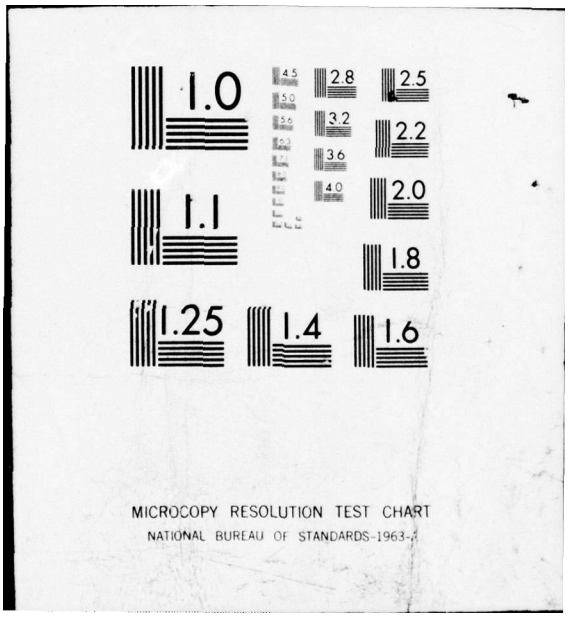
1.0
1.1
1.25
1.4
1.6
1.8
2.0
2.2
2.5
2.8
3.2
3.6
4.0
4.5
5.0
5.6
6.3
7.1
8.0
9.0
MICROCOPY RESOLUTION TEST CHART
NATIONAL BUREAU OF STANDARDS-1963-A

SYSTEMATIC SURVEY OF NAVAL SURVEILLANCE AND COMMUNICATIONS SYSTEMS

Paul Schwartz and Lynette Roth

Hughes Research Laboratories
3011 Malibu Canyon Road
Malibu, CA 90265

March 1977

Contract N00173–76–C–0389
Final Report
For Period 30 September 1976 to 31 March 1977

Approved for public release; distribution unlimited.

Sponsored by
NAVAL RESEARCH LABORATORY
Washington, DC 20375

UNCLASSIFIED

SECURITY CLASSIFICATION OF THIS PAGE (When Data Entered)

REPORT DOCUMENTATION PAGE	READ INSTRUCTIONS BEFORE COMPLETING FORM
1. REPORT NUMBER	2. GOVT ACCESSION NO. 3. RECIPIENT'S CATALOG NUMBER
4. TITLE (and Subtitle) SYSTEMATIC SURVEY OF NAVAL SURVEILLANCE AND COMMUNICATION SYSTEMS.	5. TYPE OF REPORT & PERIOD COVERED Final Report 30 Sept 1976-31 Mar 1977
	6. PERFORMING ORG. REPORT NUMBER
7. AUTHOR(s) Paul Schwartz and Lynette Roth	8. CONTRACT OR GRANT NUMBER(s) N00173-76-C-0389
9. PERFORMING ORGANIZATION NAME AND ADDRESS Hughes Research Laboratories 3011 Malibu Canyon Road Malibu, CA 90265	10. PROGRAM ELEMENT, PROJECT, TASK AREA & WORK UNIT NUMBERS
11. CONTROLLING OFFICE NAME AND ADDRESS Naval Research Laboratory Washington, DC 20375	12. REPORT DATE March 1977
	13. NUMBER OF PAGES 80
14. MONITORING AGENCY NAME & ADDRESS(if different from Controlling Office)	15. SECURITY CLASS. (of this report) UNCLASSIFIED
	15a. DECLASSIFICATION DOWNGRADING SCHEDULE

16. DISTRIBUTION STATEMENT (of this Report)

Approved for public release; distribution unlimited.

17. DISTRIBUTION STATEMENT (of the abstract entered in Block 20, if different from Report)

18. SUPPLEMENTARY NOTES

19. KEY WORDS (Continue on reverse side if necessary and identify by block number)

Josephson effect, superconductivity, communications, surveillance, radar, receivers, ditial signal processing

20. ABSTRACT (Continue on reverse side if necessary and identify by block number)

This report contains a survey of the properties of Josephson-effect devices and an evaluation of their potential utility in Naval surveillance and communication systems. Emphasis was placed on finding an existing system that could be retrofitted to improve performance. The study focused on receiver front-end characteristics and signal-processing applications. Recommendations were made for the development of a

over

DD FORM 1 JAN 73 1473 EDITION OF 1 NOV 65 IS OBSOLETE

UNCLASSIFIED

SECURITY CLASSIFICATION OF THIS PAGE (When Data Entered)

superconductive front-end for millimeter-wave applications or the development of an integrated high-speed signal-processing capability.

TABLE OF CONTENTS

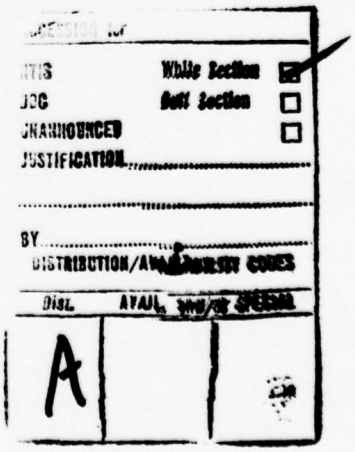

LIST OF ILLUSTRATIONS

SECTION 1

INTRODUCTION

This is the final report for Phase I of the Josephson Junction Technology Program. This phase is called the Systematic Survey of Naval Surveillance and Communications Systems. Its purpose has been to identify operational Naval systems which could benefit from a hardware retrofit utilizing Josephson-effect devices (JEDs). This retrofit, to be useful, should result in improved system performance which would extend the useful life of the system, thereby reducing the overall system life-cycle cost. Because of the difficulties that can be encountered in using a totally new technology in an existing system, NRL extended the study to include experimental systems as well as operational systems. This extension was useful because it has allowed us to make a more complete evaluation of the prospective utility of the Josephson junction technology. The survey was divided into three interactive parts:

- Survey of JED performance
- Selection and evaluation of naval systems
- Analysis of potential applications for Josephson-effect devices.

Strong interaction between the three parts of the survey was needed to complete the program on schedule. These interactions made it possible to reduce the enormous potential data base for the Naval systems to a manageable size. They also defined areas where data was lacking about specific device performance parameters, thus making a more thorough investigation of those areas possible. In spite of these efforts in the device performance survey, we were sometimes unable to find meaningful data on parameters of superconducting devices that could have a strong influence on the ultimate utility of these devices, e.g., dynamic range and damage thresholds. Therefore, these areas should receive increased emphasis in future programs to develop JEDs Further, it would be useful to fund some engineering research projects

which would focus on the utilization of reliable, manufacturable devices in a specific application where the underlying device theory has been established.

The application area which fits these requirements best is that using low-noise frequency converters or mixers. Our study has also indicated that a low-noise, millimeter-wave receiver that would use such a mixer is potentially useful in a variety of systems currently under development in the areas of high-resolution radars, missile and RPV guidance, and secure communications. Therefore, this application appears to be very suitable for development at this time.

During this first phase of the program we have conducted a thorough survey of the properties of JEDs and JED arrays. We have collected information about the observed and potential performance of these devices in the following areas:

- High-frequency radiation mixers and detectors
- High-frequency parametric amplifiers
- Superconducting quantum interference device (SQUID) amplifiers and magnetic field detectors
- Oscillators
- Digital signal processing including analog-to-digital (A/D) converters, digital logic circuits, and digital memories.

In addition to JEDs, the survey included a relatively new superconductive device, the super-Schottky, which is a competitor to the JED in mixer and detector applications.

This device survey revealed many device properties that could be useful in military applications. Two of these were (1) the potential low-noise reception of high-frequency radiation and (2) the rapid junction response time (which is useful in digital switching applications). In addition, the survey uncovered some problem areas which could reduce the utility of these devices. The most serious of these is the inherently low operating power of these devices, which places an upper limit on the size of the signal that can be processed in a linear fashion. This level is often below the power levels encountered in hostile military

environments, and it will be necessary to obtain more quantitative information on device performance at higher power levels and to investigate approaches to improving that performance (e.g., by the use of arrays).

The systems survey was performed in two stages. The first identified a very large number of systems so that all of the Navy's needs could be identified. In the second stage, a smaller list of systems was compiled, and the basic properties of these systems were cataloged for use in comparing JED capabilities with the system needs.

In the last portion of this program, we compared the needs of the systems studied with device performance capabilities revealed by the survey. For applications to existing systems the greatest potential lies in improvements to receiver performance. For atmospheric applications, environmental noise is so high and existing component performance so good that there is not much need for improvements below ~8 GHz. Above ~20 GHz or for very wideband applications, there is potential for superconducting device receivers to improve system performance. Presently, the most promising area is at millimeter-wave frequencies where current performance is significantly behind system needs. Another very promising area is in high-speed signal processing. Here we feel that the high-speed, low-power capabilities of JEDs will make practical a new generation of compact, high-speed, reliable signal-processing subsystems. These capabilities are so far beyond those of existing systems that their effect will be felt only on new system designs, where they will allow the designer to expand his horizons and realize significantly improved system capabilities.

Our recommendations for the succeeding phases of the Josephson Junction Technology Program are to give

- First consideration to the development of a low-noise, millimeter-wave reciever assembly which includes the mixer and i.f. amplifier. (A possible target frequency for the application is 94 GHz).

- Second consideration to the development of the high-speed signal-processing equipment. This task is much larger than the first one, and would therefore require more time and effort to result in a useful piece of equipment. Interim goals could be development of a 10 Gbit/s A/D converter or a small high-speed memory in ~3 years.

Finally, although it is not possible to individually acknoledge all those who contributed ideas or information to this report, we wish to thank the technical program monitor, Dr. Martin Nisenoff, for his active cooperation in helping us to obtain much of the information we used in the survey.

SECTION 2

JOSEPHSON-EFFECT DEVICE SURVEY

A. ULTRA-FAST SIGNAL PROCESSORS AND HIGH-PERFORMANCE COMPUTERS

Josephson-effect devices have shown the potential to perform significantly better than existing devices in signal processors and high-performance computers. The extremely fast switching speed and low power dissipation of JEDs lead to a power delay product which undercuts that achieved for high-frequency semiconductor devices by greater than four orders of magnitude (Figure 1).

1. Logic Functions and Switching

The low power dissipation of Josephson logic gates, e.g., < 40 nW for dc-powered non-latching quantum interference devices,[1] removes the limit on packing density encountered in advanced semiconductor circuits due to heat removal problems. Specifically, heat dissipation sets the following limit on their spacing:

$$a^2 > P/Q_m ,$$

where a is the distance between circuits arranged in a square lattice, P is the power dissipation per circuit, and Q_m is the maximum heat transfer from circuit to liquid coolant.[2] Fast semiconductor devices such as the GaAs FET and transferred electron devices (TEDs) consume power in the 10 mW range.[3] Using common coolants, e.g., Freon-113 with $Q_m = 20\ W/cm^2$, these devices must be spaced greater than 100 μm apart to avoid destructive thermal interactions; on the other hand, JEDs ($P \sim 40$ nW), which are cooled by liquid helium ($Q_m = 0.8\ W/cm^2$), can be packed as close as 2 μm without thermal degradation. The smaller spacing between JEDs reduces the signal propagation delay, thus increasing the potential data processing rate in applications where a large signal-processing capability is needed in minimal volume.

Basically, the Josephson tunnel junction operates as a fast switch in which the current can be carried in either of two voltage states, i.e., zero or finite voltage corresponding to the superconducting energy

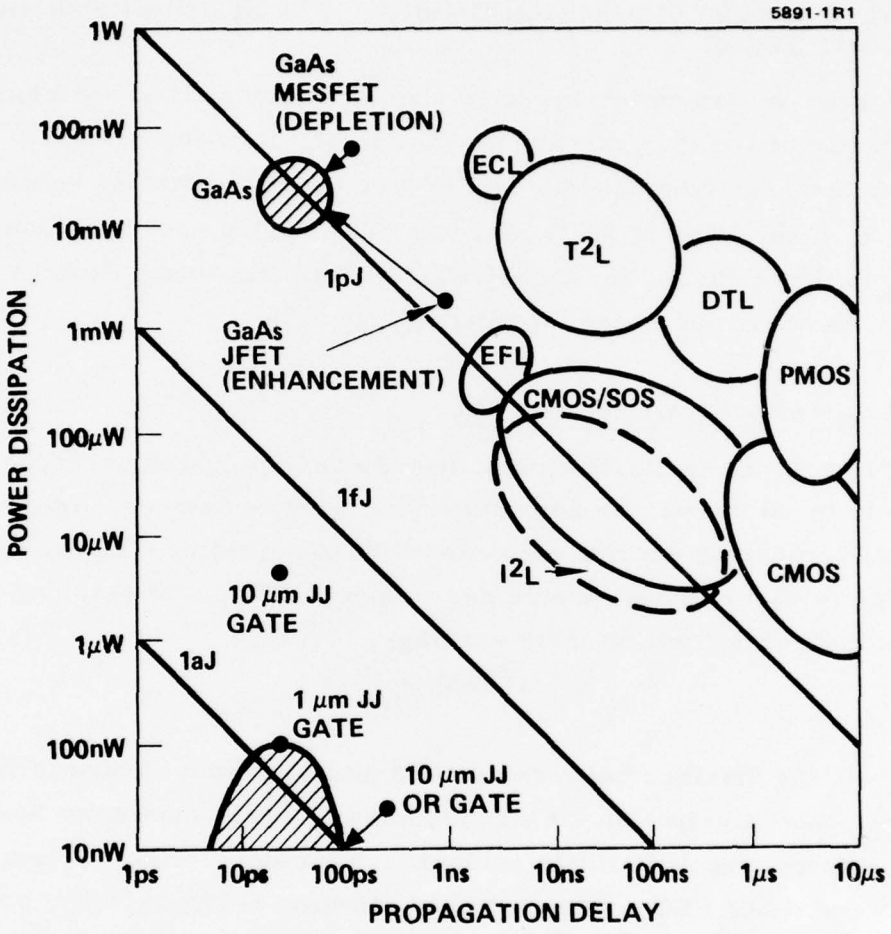

Figure 1.
Power dissipation versus propagation delay product for competitive logic gate technologies. Thermal noise is approximately 10^{-21} J at room temperature and 5×10^{-23} J at 4 K.

gap, 2Δ. The strong dependence of the zero-voltage current on magnetic field provides the mechanism for transitions between states. Measurement of the switching transient (from zero to the gap voltage) of a small, high-current-density junction has determined an upper bound of 38 ps for the risetime.[4] A still smaller value, viz., near 6 ps, is expected if test-chip reactances are eliminated.* The power dissipation, determined by the product of the theoretical Josephson current for the junction and its on-state voltage $2\Delta/e$, is 100 nW. Thus the power-risetime product is extremely small, i.e., $< 3.8 \times 10^{-18}$ J.

In a recent paper,[1] H.H. Zappe discussed the logic delay for two Josephson devices, i.e., in-line gates and quantum interference devices, and has compared the effect of their miniaturization on ultimate speed and power level in Josephson circuits. He defines the logic delay, D, as the time interval between the moment at which the circuit begins to switch into the voltage state and the time at which the last gate driven by the circuit begins to switch. The total time delay has three principal components: (1) the risetime of the output current, which is determined by the voltage transition of the junction; (2) a fan-out delay which occurs due to the presence of inductive discontinuities; and (3) the delay in the transmission line. For any given inductive discontinuity, transmission line length, and junction size, the logic delay can be minimized by adjusting the line impedance Z_o; the risetime dominates for large Z_o and the fan-out delay controls the small Z_o case.

To achieve higher circuit densities for future miniaturized circuits, the width of transmission lines (and junctions) must decrease. To maintain the threshold curves for the in-line Josephson gate, the junction length must remain constant as the width decreases. Briefly, the risetime of the output current remains nearly constant as the circuit shrinks and ultimately limits the logic delay. Present logic devices, using in-line gates, have exhibited logic delays of ~170 ps at power levels of 28 μW (Ref. 16). According to the previous discussion, these devices cannot be miniaturized enough to bring dramatic improvements in speed or reductions in power. However, a recent Josephson circuit,

*Recently, switching speeds below 10 ps have been measured.[5]

the quantum interference device, has been developed that lifts the restrictions on the geometry of the in-line device required to shape the threshold curve. Hence the quantum interference device can be shrunk in both length and width, resulting in increased speed and lower current (and power) levels. A more detailed analysis of the factors limiting the size and speed of these devices remains a significant open question in the literature.

Simple logic functions have been performed with three-junction interferometers.[1,6] Five OR circuits connected in series, four non-latching stages followed by one latching stage, were tested. The logic delay was found to be 235 ps/stage and the power dissipation was ~40 nW in continuous operation: the corresponding power-delay product for these circuits is 7×10^{-18} J. These devices had comparatively gross dimensions: a 51 μm x 269 μm gate area containing 9 μm x 11.5 μm junctions and 76 μm wide transmission line interconnections. Both speed and power levels will improve with higher resolution and circuit density. The reduced capacitance and Josephson threshold current of these devices allow them to be operated as non-latching logic circuits.

2. Memory Elements and Storage

In this section we will discuss two approaches to achieving memory and storage with Josephson gates. Both approaches rely on the quantization of current circulating in a superconducting loop. This current, quantized in units of Φ_o/L where L is the inductance of the superconducting ring and $\Phi_o = 2.07 \times 10^{-15}$ Vs (a small value), makes stable, low-current devices possible.

The first concept for a memory cell, proposed by Anacker,[8] consists of two in-line junctions in a superconducting loop to perform the writing function and a third Josephson gate to sense or readout non-destructively. Information is stored as clockwise or counterclockwise circulating currents in the loop. Writing is accomplished by the coincident application of current (1) in the word line, which is fed through the memory loop, and (2) in the overlaid bit line, which produces a magnetic field at the gate. The polarity of the bit current selects the

gate to be switched, hence the direction of the circulating current after the write cycle. The operation of this cell lends itself to use in a bit-organized memory array.

A sense gate, placed near one branch of the memory cell, switches into the voltage state only if the cell contains circulating current of the proper polarity. This process accomplishes readout nondestructively. The cell to be interrogated is selected with coincident word and sense currents. In a bit-organized array, these sense gates are connected serially in the bit direction.

The feasibility of this basic memory cell concept has been demonstrated experimentally by Zappe.[9] He achieved a switching time of 600 ps for a minimum line width of 2 mil (50 μm) and a cell area of 500 mil^2 using a miniaturized version of the loop-memory cell. Broom et al.[10] made smaller versions of this memory cell (1.4 mil^2) which they operated with a 2 μs cycle time. They also measured current transfer times in the cell less than 80 ps. The energy dissipated during switching is estimated to be about 10^{-16} J. These small-area cells, e.g., A = 1.4 mil^2 (875 μm^2), were fabricated with 2 μm minimum linewidth. They contained Josephson junctions with dimensions 5 μm x 5 μm, which carried the high Josephson current densities (e.g., 30 kA/cm^2) required for small-area cells.

The second concept involves the storage of information in the form of single flux quanta, Φ_o. This stored energy is given by $\Phi_o^2/2L$, typically on the order of 10^{-18} J. One device which performs this junction is a two-junction interferometer: in the simplest form it consists of two point junctions and an inductance L in a superconducting loop. The control characteristic of this device has overlapping lobes, corresponding to vortex modes which are either empty or contain, clockwise or counterclockwise, circulating currents. The interferometer has memory by virtue of the vortex mode overlap.

Two methods of readout, both destructive, have been explored. Guéret[11] has shown that the energy released by expelling a single flux quantum from a memory cell can be detected with a sensitive Josephson

circuit. The second method involves switching the device out of the superconducting state into a voltage state.[12] Applying appropriate coincident word (gate) and bit (control) currents, the memory cell switches to the gap voltage if a single flux quantum was stored and remains in this state until the word current is removed. This provides a considerably larger amount of energy to external sense currents than that originally stored in the device.

The switching speed for the vortex-to-vortex transition has been measured for a small, two-junction, quantum-interference device. The measured risetime of 100 ps is larger than the computer value of about 50 ps, probably because of chip-and-holder parastics.[13] The area of this interferometer is 150 μm^2; the dimensions of the junctions and inductance are (4 x 7) μm^2 and (6 x 7) μm^2, respectively; and the control line width is approximately ~2 μm.

The basic building block of a memory array using these devices is an array of these single-flux quantum (SFQ) cells, connected serially to form a string, driven by the word current. A number of such strings in parallel would make up the array. Computer simulations have indicated that strings of SFQ cells can operate safely.[13]

3. Large Memory Circuits

Using the non-destructive readout (NDRO) memory cell, which contains in-line Josephson gates, Anacker[8] designed two random-access memory modules: a tree-type decoder with cross-control gates and a decode, bit, and sense circuit for a bit-organized memory. Subsequently Zappe[9] demonstrated experimentally that these memory cells may be used to build high-speed memories, requiring zero standby power. In this work, large cells (20 mil x 25 mil) produced, as expected, rather slow current transfer times (600 ps) and dissipated 2×10^{-15} J/write cycle. (Compare these values with the parameters for the 1.4 mil^2 cell discussed in 2.A).

As expected for a quantized system, the memory demonstrated remarkable stability. Even during sensing in a word-selected memory cell, the stored flux was not altered by a single flux quantum after 5×10^8 NDRO cycles. The operating margins measured without word, bit, and sense disturbs, allowed independent variations in word, bit, and sense currents of ± 11.5%, ±26%, and ±15%, respectively. Recently, Henkels and Zappe have announced an experimental 64-bit decoded, Josephson NDRO, random-access memory.[14]

4. Complex Logic Circuits

Complex experimental logic circuits have been built using Josephson junction circuits. For instance, Herrell has designed, fabricated, and evaluated a 4-bit multiplier circuit based on in-line Josephson tunneling logic (JTL) gates[15] (see 2.A.1). These devices consist of a multi-control Josephson tunneling gate driving a pair of transmission lines of characteristic impedance Z_o terminated in a resistance R. In this case, the transmission line was not terminated in its characteristic impedance, i.e., $R \neq 2Z_o$, but was deliberately mismatched by choosing $Z_o = 3$ R, the value yielding an optimum design trade-off between logic delay (a minimum in the matched condition) and gate string disturbances. In earlier work, Herrell had shown that, through a suitable choice of Josephson junction characteristics, biases, current levels, and polarities, the basic Josephson tunneling gate can perform the logic functions, AND, OR, and CARRY.[16] A simple logic circuit involving three OR gates and an AND gate was fabricated using a comparatively gross, minimum-linewidth technology of 1 mil (25 μm). The circuit operated with an average delay of 170 ps per logic gate, which, with an average power dissipation of 28 μW, corresponds to a power-delay product of approximately 5 femtojoules (50% duty cycle). Miniaturization may reduce the values for gate delay and power dissipation substantially for circuits using in-line JTL and even more dramatically in those based on quantum interference devices (Section 2.A.1).

Herrell demonstrated that these superconducting logic circuits can successfully be extended in complexity, e.g., to operate as a four-bit multiplier.[15] His multiplier circuit combined the elements of an adder, a shift register, and a control circuit. The algorithm adopted for the circuit was that of a simple serial 4-bit multiplier consisting of a 4-bit adder with ripple carry, together with a 4-phase, 8-bit accumulator shift register. The circuit, fabricated using the proven 25 μm linewidth technology, operated with a minimum cycle time of 6.67 ns (150 MHz), a limit imposed by the external test equipment, and gave a 4-bit multiplication time of 27 ns (4 cycles). With better external pulse generators or with internal Josephson junction generators, computer simulations indicate a 3 ns cycle time giving a 4-bit multiplication time of 12 ns. The average loaded logic delays were measured to be 236 ps/gate and 275 ps/gate for fan-outs of 1 and 4, respectively. The overall power dissipation level of the complete multiplier was estimated to be 1.57 mW, corresponding to 35 μW/gate including power-string resistor dissipation.

5. A/D Converters

An experimental A/D converter using integrated Josephson junction circuits has been reported.[17] This fast data acquisition circuit was designated to operate compatibly with high-performance Josephson junction computers. The converter consists of a sample-and-hold circuit and a 4-bit successive approximation A/D unit integrated on a 6.25 mm square chip. The sample-and-hold function is performed by a Josephson-junction switch across a superconducting loop, and the conversion circuit uses multi-control, in-line Josephson gates.

The A/D circuit, fabricated with 25 μm minimum linewidths, yielded an analog signal bandwidth capability of 25 MHz, limited by the risetime of the sample control pulse from an external generator. Circuit simulations had predicted a bandwidth of 35 MHz. The key parameter in any A/D scheme is the switching speed of the circuit which determines the data processing rate. Microscopic analyses of JEDs have shown that picosecond voltage pulses can be developed by these

devices.[18] Assuming 10 sequential operations must be performed during each cycle, these switching speeds project a conversion rate approaching 20 GHz.

B. HIGH-FREQUENCY SUPERCONDUCTING DEVICES

In this section, we will discuss the performance of superconducting devices as mixers, detectors, and parametric amplifiers at microwave, millimeter, and submillimeter wavelengths. Emphasis will be placed on the device characteristics most important in these applications, i.e., sensitivity, bandwidth, and dynamic range. Additionally, we will describe the use of series arrays of JEDs to obtain improved device performance. Finally, JED arrays are examined as candidates for high-frequency sources, e.g., wide-band, voltage-controlled microwave oscillators.

1. The Super-Schottky Diode and the Josephson-Effect Mixer

The need for sensitive receivers in the millimeter and submillimeter wavelength range has stimulated extensive work on Josephson-effect mixers. Table 1 compares the performance of these mixers in various modes as well as that of the super-Schottky and conventional Schottky mixers. Figure 2 presents the input noise temperatures for competitive high-frequency receivers. The performance numbers listed in this section must be considered as approximate guidelines for real applications since they are often derived from very different types of measurements. Some are calculations of the mixer contribution to an overall receiver, where it is often impossible to establish the performance of individual components accurately; others are laboratory measurements of mixer noise in configurations which are unlike those encountered in real applications.

For higher frequencies, the device sensitivity, which is limited by internally generated noise, has been related to an equivalent noise temperature which can be used to compare the utility of different devices in a particular application. The noise temperature is defined in the following manner. When a receiver is connected to an antenna

Table 1. Comparative Performance of High Frequency Mixers

Mixer			Input Mixer Noise	Conversion Gain	Frequency and Bandwidth			Saturation Level, W	P_{LO}, W
	Ref	Temp, K	T_M (meas.), K		f_s, GHz	f_{if}, MHz	Δf_{if}, MHz		
Josephson mixer: fundamental, external LO	19 20	1.4	54	1.35	36	50	20	10^{-10}[a]	10^{-8}
	22	4	7×10^{5} (7000)	10^{-3} (0.2)[b]	891	.01-1			10^{-7}
Josephson mixer: harmonic external LO	53	7	400	0.5	36	50	20		
Josephson mixer: internal LO	54	4	100-600	0.06	206	60 280	400		
Super-Schottky	21	1.1	6	0.18	9	1400		10^{-9}[c]	2×10^{-8}
Cooled Schottky	55	18	280	0.42	85	1400	60		10^{-3}
Room temperature	56	300	5000		340	2300		10^{-4}	50×10^{-3}
Schottky	57		950	0.32	60	1200	600		5×10^{-3}

[a] Experiments have indicated as the output saturate for an input signal of approximately 10^{-2} P_{LO}.
[b] Corrected parameters, assuming input coupling of unity.
[c] Estimated saturation level, calculated in text.

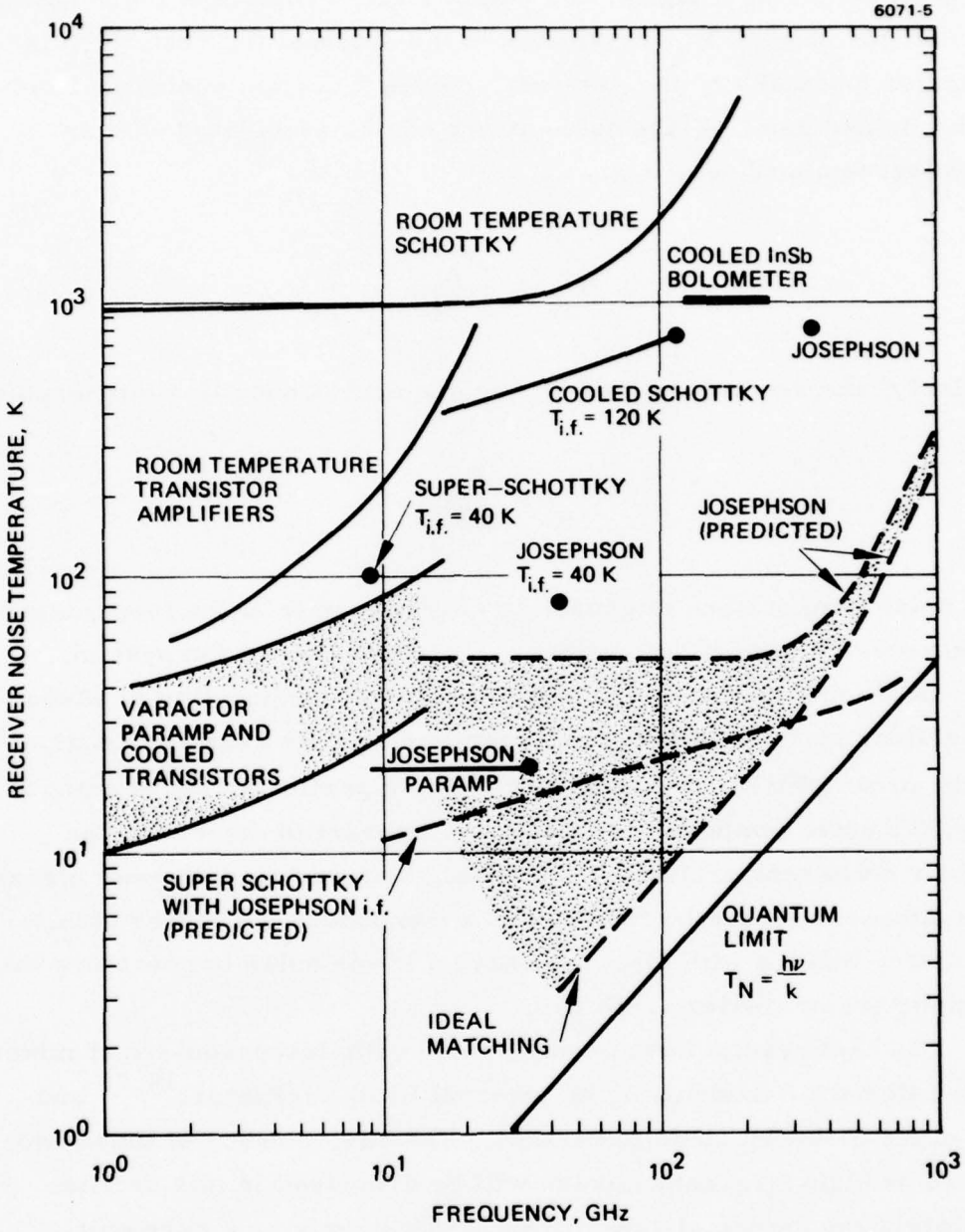

Figure 2.
Comparison of input noise temperatures for high-frequency receivers. Projected performance for superconducting receivers is indicated by dashed curves.

but is not receiving a signal, the output signal consists of noise power. Some of this power, P_A, originates in the antenna; the rest, P_R, is generated internally to the receiver. Given a certain operating bandwidth, B, and gain, G, the noise power can be associated with an equivalent temperature, e.g.,

$$T_A = \frac{P_A}{kBG} .$$

Similarly, the receiver is said to have an equivalent noise temperature

$$T_R = \frac{P_R}{kBG} .$$

This noise temperature is generally characteristic of the input stages of the receiver, and it defines the basic sensitivity of the system.

Depending on the design of the receiver, it is possible to associate portions of T_R with different components in the receiver, e.g., mixer, preamplifier, i.f. amplifier. For a particular set of components, the noise temperatures and gains interact to determine the receiver noise temperature. In general, however, a somewhat higher noise temperature can be tolerated if a component has larger gain. Therefore, mixers with loss must have a lower noise temperature than do amplifiers or mixiers with gain.

The best results have been obtained with Josephson-effect mixers in the heterodyne mode using an external local oscillator,[19,20] and with super-Schottky diode mixers.[21] The performance of these two devices as high-frequency mixers will be discussed in this section. The Josephson device also performs impressively as a harmonic mixer, e.g., down-conversion from 891 GHz with a 1 GHz external local oscillator has been observed.[22] The Josephson mixer, which generates its own local oscillator power, may be useful at submillimeter and infrared frequencies, where sources are difficult to implement. However, the Josephson oscillator linewdiths, e.g., 1 GHz, limit the

internal local oscillator mode to applications with relatively high frequency, wide band i.f. amplifiers, and a tolerance for high local oscillator noise.

a. The Super-Schottky Diode

The super-Schottky barrier diode, a superconductor-semiconductor tunneling junction, has achieved the lowest input-noise temperature, i.e., 6 K at 9 GHz, of any mixer reported in the literature.[21] Additionally, it possesses a bandwidth far wider than the best available parametric and maser amplifiers with comparable noise temperatures. However, since this mixer has loss rather than gain, the overall receiver performance depends critically on the i.f. amplifier. Low-noise masers or paramps may be used, although they may limit the bandwidth. An externally pumped, Josephson up-converter paramp might also prove successful.

The super-Schottky mixer, similar to conventional Schottky diodes, achieves high performance as a result of the nonlinearity in its (I, V) characteristic. Although the physical mechanisms underlying their nonlinearities are different, the (I, V) behavior of either diode can be expressed approximately by $I = I_o \exp(SV)$, where I_o is determined by the area and material parameters of the diode and the parameter S is a measure of its nonlinearity. The parameter S is given approximately as $S \simeq q/k(T + T_o)$, where q is the electronic charge, k is the Boltzman constant, T is the temperature, and T_o is an empirical constant. For super-Schottky diodes, T_o is less than 1 K; for conventional Schottky barriers on GaAs and Si, T_o is greater than 40 K. Thus, super-Schottky diode mixers operating at 1 K may show greater than 40 times improvement in noise temperature.

The central parameter S controls the receiver performance through the input noise temperature, T_r, and the dynamic range. The receiver noise temperature can be expressed as $T_r = L_c(T_D + T_{i.f.})$, where L_c is the single-sideband conversion loss of the mixer, T_D is the noise temperature of the mixer at the i.f. terminals, and $T_{i.f.}$ is the

noise temperature of the i.f. amplifier. The conversion loss is often taken as the product of two terms $L_c = L_l$, where L_o is the intrinsic conversion loss associated with frequency conversion in the nonlinear resistance and L_l is the loss arising from parasitics. It can be shown that L_o decreases as SV_l increases, where V_l is the amplitude of local oscillator voltage. For super-Schottky diodes, the swing of LO voltage is limited to the range 0 to Δ, where Δ is the superconducting gap parameter. This limits the intrinsic conversion loss of the super-Schottky diode. Furthermore, care must be taken to minimize leakage currents, which reduce the range over which S is constant. Lower temperatures and larger-gap superconductors can also result in reduced conversion loss.

An intrinsic conversion loss of 4.9 dB was deduced from the 0.9 K I-V characteristic of a Pb on p-GaAs super-Schottky. Parasitic loss due to the junction capacitance and spreading resistance contributes an additional conversion loss L_l. Presumably, several techniques can be employed to minimize this loss, e.g., thinning the semiconductor.[23]

The magnitude of the S value and its constant range determines the saturation level and dynamic range of this device. For example, consider a mixer diode with $S = 4000\ V^{-1}$, $\Delta V = \Delta/2$ ($2\Delta = 2.73$ meV for Pb); and $R_d = 400\ \Omega$, where R_d is the resistance at the signal frequency. This mixer should saturate severely at

$$P_s = P_{LO} \simeq \left(\frac{\Delta}{2}\right)^2 / R_d \simeq 10^{-9}\ \text{W}.$$

Assuming the minimum detectable power for the mixer is $P_{min} = kT_M B$ where B is the bandwidth, we find $P_{min} \simeq 10^{-13}$ W for $T_M = 6$ K and B = 1 GHz. Thus, the dynamic range is only about 10^4 or 40 dB.

b. The Heterodyne Josephson-Effect Mixer

Josephson junctions as heterodyne detectors have been extensively investigated, experimentally and theoretically.[19,20,24,25] The principle of detection with Josephson junctions relies on the fact that the relation between current and voltage for an ideal Josephson element is highly nonlinear. In contrast to the super-Schottky, which can be thought of as a non-linear resistance, the Josephson junction behaves as a lossless nonlinear inductor, generally useful for high-frequency device applications.

In the heterodyne mode with an externally applied local oscillator,[26] a small signal is mixed with a relatively large LO signal in the junction to produce an output at the difference frequency much lower than the signal frequency. Calculations based on the resistivity shunted junction (RSJ) model predicted that small-signal conversion gain ($n = L_1^{-1} > 1$) can be achieved in a Josephson-effect mixer at values of the normalized frequency $\Omega = h\nu/2eI_cR \ll 1$, where ν is the signal frequency, I_c is the Josephson critical current, and R is the shunt resistance. (If $\Omega > 1$, the conversion loss increases as Ω^2.) Furthermore, the RSJ model shows the noise temperature of the Josephson mixer to be $T_M = 30\ \Omega T$ for $0.1 \leq \Omega \leq 1$, where T is the ambient temperature in Kelvin. Since the theoretical limit for the I_cR product is $\pi\Delta/2e$, ideal Nb junctions should have $\Omega = 1$ at a signal frequency $\nu = 1$ THz, thus $T_M/T \approx 30\nu$ (ν in THz) for $0.1 \leq \Omega \leq 1$.[26]

The mixer performance at 36 GHz of point-contact JEDs made with several different superconductors have demonstrated good agreement with the theory. For example, operating vanadium-point contacts at 1.4 K, Taur, Claassen, and Richards have achieved a single-sideband mixer noise temperature of 54 K with a conversion gain of 1.35 and a signal bandwidth on the order of 1 GHz.[24] Although the noise of this mixer is greater than that of the super-Schottky diode, the Josephson mixer has the advantage of conversion gain, which reduces the contribution to the receiver noise temperature from the i.f. amplifier noise. Figure 3 demonstrates the importance of minimizing the

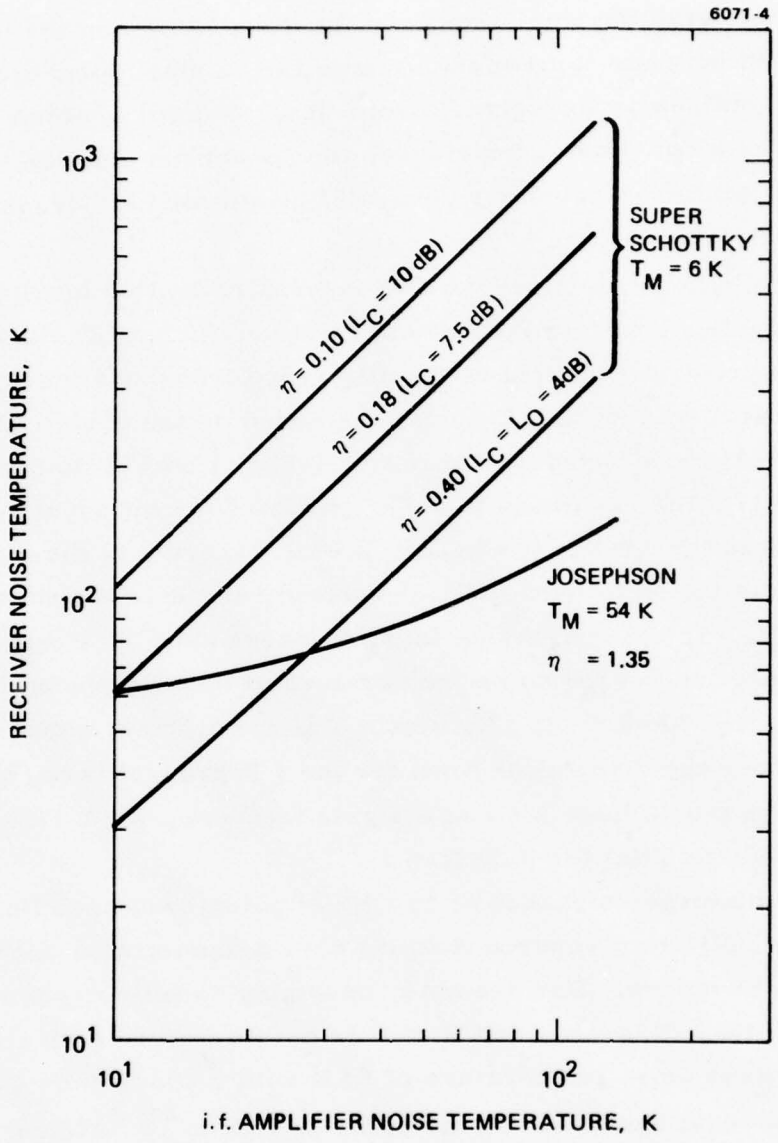

Figure 3.
Effect of mixer conversion loss on receiver noise temperature as a function of i.f. amplifier noise.

conversion loss in the mixer diode. For the super-Schottky diode a conversion loss of 4 dB corresponds to the theoretical lower limit for intrinsic loss for lead contacts at 1K.[21,27]

The dynamic range of the Josephson mixer shares the problem of low saturation power level with the super-Schottky. Experiments have shown that the i.f. output saturates for a signal power comparable to $10^{-2}\ I_c^2 R$ with local oscillator power $P_{LO} \simeq I_c^2 R$. This number is on the order of 10^{-10} W. Although the low saturation level places a rather severe restriction on the dynamic range, the use of arrays may improve this parameter (see 2.B.4.a).

2. Detectors

The search for sensitive, high-speed detectors for submillimeter and infrared frequencies has provided impetus for the effort to develop Josephson video detectors. In Table 2 we present a summary of their performance along with the parameters of competing devices, i.e., bolometers and Schottky diodes. Both broadband[28] and tunable narrow-band[29] Josephson detectors have been developed. A wide-band detector based on high-performance (100 Ω to 1000 Ω) point contacts has sensed radiation from a 300 K source with an estimated NEP = 3×10^{-15} W/Hz$^{1/2}$ (Ref. 30). The response of niobium point contacts has been found to extend to frequencies greater than 1.2 THz ($\lambda < 250$ μm). The feedback-narrowed (regenerative) detector has been used to make radio-astronomical observations at 1 mm wavelength.[31]

Comparing the performance of Josephson video detectors with bolometers, we note that the principal advantage of the former class is its high response speed. Actually, for wavelengths shorter than 1 mm ($f > 300$ GHz), the bolometers should have better sensitivities than those of Josephson video detectors, because the noise equivalent power (NEP) of a Josephson detector is proportional to the square of the signal frequency. The super-Schottky diode may compete with either bolometers or Josephson detectors if the performance reported at 9 GHz can be achieved at higher frequencies.

Table 2. Performance of High-Frequency Radiation

Detector	Ref.	Temp, K	Sensitivity, $W/\sqrt{Hz}$		Frequency and Bandwidth		Dynamic Range	Comments
			Measured	Theoretical	f_s, GHz	Δf, GHz		
Josephson, broadband	28	4	5×10^{-15}	8×10^{-16}	90		>30 dB	Response time $\tau < 10$ ns
	30	1.8	3×10^{-15}	10^{-16}	120	40		300 K source
Josephson, narrow band regenerative	29		$<10^{-14}$	3×10^{-16}	187	<0.30		Tunable
Josephson SNS bolometer	58	1.5	5×10^{-15}	1×10^{-15}				$\tau = 0.1$ s
Superconducting transition edge bolometer	59 60	1.5	2×10^{-15}					$\tau = 0.1$ s
Ge bolometer	61	4	10^{-13}					$\tau = 0.01$ s
Super-Schottky	21	1.1	5.4×10^{-16}		9			
Schottky	62	300		4.5×10^{-13}	10			
		77		2.5×10^{-15}	10			

3. Amplifiers

Table 3 compares the performance of the following Josephson-effect amplifiers: a four-photon externally-pumped amplifier and three-photon, self-pumped parametric amplifiers in the single-idler, double-idler, and upconverter modes. The Josephson parametric amplifier uses the nonlinear inductance of a Josephson junction as the active element; in comparison, the conventional parametric amplifier relies on the nonlinear capacitance of a varactor diode. The unbiased Josephson junction, the active element in the four-photon amplifier mode, is symmetric with a physical inversion. As a result, the nonlinear inductance depends only upon even powers of current, thus even harmonics are absent in the voltage output, i.e., no dc-rectified or second-harmonic voltages and no voltages at the sum or difference frequencies. This mode simplifies the required circuitry: (1) the signal (ω_s) and idlers (ω_i) are simply sidebands of the pump (ω_p) allowing all three frequencies to be handled by the same circuit, viz., $2\omega_p = \omega_s + \omega_i$ and $\omega_p \approx \omega_s \approx \omega_i$; (2) the elimination of parasitics is simplified, since parasitics at even harmonics are absent; and (3) electrical leads are not required for the unbiased function. These amplifiers have been fabricated using a series array of Dayem bridges,[32] a series array of tunnel junctions,[33] and a single point contact.[34] The performance of the microbridge array is discussed in 2.B.4.b. Briefly, this device possesses the desirable characteristics of high gain, wide bandwidth, low noise, and low pump power; a drawback is its low saturation level.

Self-pumped parametric amplifiers have been operated in the following modes: single-idler, negative-resistance amplification; two-idler, negative-resistance amplification; and parametric up-conversion. The second mode appears promising for frequencies above 100 GHz, because the relatively large noise temperature reaches a minimum (42T) at $\Omega = 1$ (Ref. 35). In the up-converter, gain is achieved by the fact that reactively stored power in the Josephson device is proportional to the frequency. This parametric up-converter can be coupled with a low-noise down-converter to provide low-noise single-frequency amplification.[36]

Table 3. Performance of Josephson-Effect Amplifiers

Amplifier	Ref.	Temp, K	Sensitivity		Frequency and Bandwidth		Dynamic Range	Pump Power, W
			Gain, dB	Noise, K	f_s, GHz	Δf, GHz		
Four-photon parametric: external pump	32	2.9	15	20 ± 10	33	>3.4	7	5×10^{-8}
			38			0.004		
Three-photon parametric: self-pumped	63	2.4	12	<20	10	1		1.7×10^{-7}
Single-idler	64	4.2	11		9	0.01		
Two-idler	35	4.2	20	200	9	0.008	<40	
Parametric up-conversion	64	4.2	14	<15	0.115	0.001		

4. Series Arrays of JEDs in Millimeter-Wave Applications

In an excellent review article, P. L. Richards has discusssed many advantages of series arrays of JEDs in millimeter-wave applications.[37] He has described successful use of arrays in an externally pumped, Josephson-effect parametric amplifier (also discussed in our first bi-monthly report) and has speculated on the potential performance of arrays as video detectors, heterodyne mixers, and internally pumped parametric amplifiers. In addition to these applications, other groups have shown that arrays are good candidates for wide-band, voltage-controlled microwave sources.

a. Mixers and Detectors

For heterodyne mixers with an external local oscillator and for video detectors, arrays of JEDs with critical currents which differ by only a few percent should be useful.[37] The requirement of junction uniformity for these applications, determined by dc bias conditions, is less stringent than it is in applications where the value of the Josephson frequency is crucial, i.e., internally pumped mixers and amplifiers as well as microwave sources.

A series array should solve many problems in mixer and detector design and should improve their performance. First, these devices share the common problem of matching to the high impedance of a space wave at microwave frequencies. The predicted value of mixer noise temperatures can only be approached under ideal matching conditions. With nonideal matching, Richard's analysis predicts a mixer noise temperature of $T_M \approx 30T$ throughout most of the millimeter-wave spectrum rather than $T_M/T \sim \nu$, where ν is the frequency in GHz, which is the case for optimum coupling.[37]

Preliminary measurements on radiation sensors have demonstrated that the higher resistance of a proximity bridge array in comparison with that of a single junction is helpful in matching to higher-impedance radiation sources. For example, placing a 10 Ω array in an X-band waveguide circuit results in the absorption of 30% of the incident power by the array. Also series arrays improve the performance

of mixers by eliminating the hysteresis in their (I, V) characteristics arising from the matching circuit.[37] According to the RSJ theory, if the circuit impedance is high at all frequencies, then the (I, V) characteristic is hyperbolic rather than hysteristic. This criteria is satisfied for series arrays, because each junction looks into the high impedance of other junctions. Finally, the crucial problem of low saturation level of Josephson mixers may be alleviated by the use of a high-impedance series array, because the power in each junction would be reduced.

b. Amplifiers

Series arrays have performed well in externally pumped Josephson-effect parametric amplifiers. These amplifiers operate in the doubly degenerate negative-resistance mode in which the junction has zero dc, current and voltage, bias. This bias mode circumvents the requirement for uniform junction properties which are needed to achieve a uniform bias condition which is necessary in other applications. Amplifiers have been operated at 10 GHz and 33 GHz using microbridge arrays[32] and at 9 GHz using tunnel junction arrays.[33]

The use of arrays solves two important problems in the design of this type of amplifier. First, the coupling between the active element and the external load can be optimized by increasing the impedance of the linear series of devices to a value greater than the transmission line (load impedance), e.g., an array of 100 microbridges each with a shunt resistance of 1 Ω exceeds a typical transmission line impedance of 50 Ω. Second, where the maximum allowable noise power background before amplifier saturation should occur depends on N^2, where N is the number of junctions in the array. Thus the gain-bandwidth product for the amplifier increases for amplifiers using arrays, because the saturation level is raised and bandwidths, restricted to avoid saturation, may be widened. Using arrays of 100 microbridges, values of 12 dB to 15 dB gain with 1 GHz and 3.4 GHz bandwidths at 10 GHz and 33 GHz, respectively, have been observed. The dynamic range of these amplifiers is relatively small, limited at the small signal end by amplification of junction noise. Upper limits to the noise of the amplifier operated with a cooled circulator have been set around 20 K.

c. Sources and Oscillators

Theoretically, Tilley has predicted that m identical junctions connected in series can interact with a cavity mode so that the number of coherently emitted photons is proportional to m^2. Therefore, much interest has developed in using series arrays of Josephson junctions as microwave and millimeter-wave sources. The first direct observation of coherent radiation from coupled Josephson junctions was made by Finnegan and Wahlsten.[38] They reported that the microwave power of two waveguide-coupled, self-resonant Josephson junctions, connected in series, was four times that from a single junction. This result directly demonstrated the super-radiant state for a pair of junctions. Furthermore, the linewidth of the detected radiation was less than 5 kHz, the minimum linewidth their measurement could resolve. The maximum microwave power detected from a pair of coupled junctions was 2×10^{-10} W at 9.1 GHz.

Further studies with stripline-coupled junctions have demonstrated frequency-pulling and coherent locking for two-[39] and three-[40] junction arrays. Microwave power ($\sim 10^{-12}$ W) was detected at 4, 8, and 12 GHz. Problems in matching stripline impedance partly account for the lower power: for single junctions, maximum powers at X band of 10^{-11} W have been observed for stripline coupling, while 10^{-9} W at 9 GHz has been achieved for waveguide coupling. Injection-locking experiments, with an external microwave source at or near the resonant frequency of the unperturbed Josephson oscillator (e.g., 4 GHz), have shown coherent locking for frequency differences between two individual radiating junctions as large as 10 MHz and significant linewidth reductions.[39]

Currently, a major goal in superconducting device applications is to develop a voltage-controlled microwave source such that the output frequency is linearly proportional to the applied voltage over multi-octaves of frequency, viz., a voltage-controlled oscillator (VCO). One approach employs a series array of microbridges rather than tunnel junctions, as the latter generally have internal resonances due to their higher capacitance. When the spacing between the elements of the

array is made sufficiently small, i.e., less than a few microns, the junctions lock in a synchronous state without either a resonant cavity or external radiation.[41,42] As part of an ongoing effort to achieve a VCO with a useful power output, a single, bare microbridge (outside a resonant cavity) has been used to produce microwave power (~10^{-12} W) which is voltage-tunable from 2 to 12 GHz.[43] Linewidths for these devices are larger than 100 MHz. In addition, voltage-locking (identical nonzero dc voltage across each junction) between two series-connected microbridges in close proximity has been observed over >40 μV; this is an indication that synchronous radiation may be achieved from microbridge arrays.

C. SQUIDs FOR LOW-FREQUENCY APPLICATIONS

For the measurement of small changes in magnetic field and small voltages, superconducting quantum interference devices (SQUIDs) clearly outperform their competition. These measurements are accomplished by two basic SQUID types: (1) the dc SQUID, which consists of two Josephson junctions placed in a superconducting ring of inductance L; and (2) the rf SQUID, which consists of a superconducting ring containing a single junction which is weakly coupled to the coil of a tank circuit. The double-junction device exhibits a dc Josephson effect, i.e., the critical current of the two junctions is periodic with respect to the magnetic flux applied to the ring, while the rf SQUID requires ac modulation to achieve its sensitivity to changes in magnetic flux.

Figure 4 compares the noise power spectra measured for a dc SQUID and several rf SQUIDs pumped at various frequencies. These SQUIDs operate in a feedback mode, i.e., in a flux-locked loop. The figure of merit shown is the energy resolution appropriate for low-frequency applications which require coupling to a superconducting transformer. The energy resolution per hertz referred to the input coil of inductance L_i coupled to the SQUID is

$$\frac{S_\phi}{2M_i^2/L_i} = \frac{S_\phi}{2\alpha^2 L} ,$$

where S_ϕ is the power spectrum of the flux noise and M_i is the mutual inductance between the SQUID and input coil. Figure 4 shows the corresponding flux noise power spectra for these SQUIDs.

Clark, Goubau, and Ketchen[44] have developed the most sensitive dc SQUID. The performance for this SQUID, used in the feedback mode and transformer-matched to the output preamplifier, is characterized by the following parameters: (1) in the white-noise region, energy resolution of 7×10^{-30} J Hz^{-1} or rms flux noise of

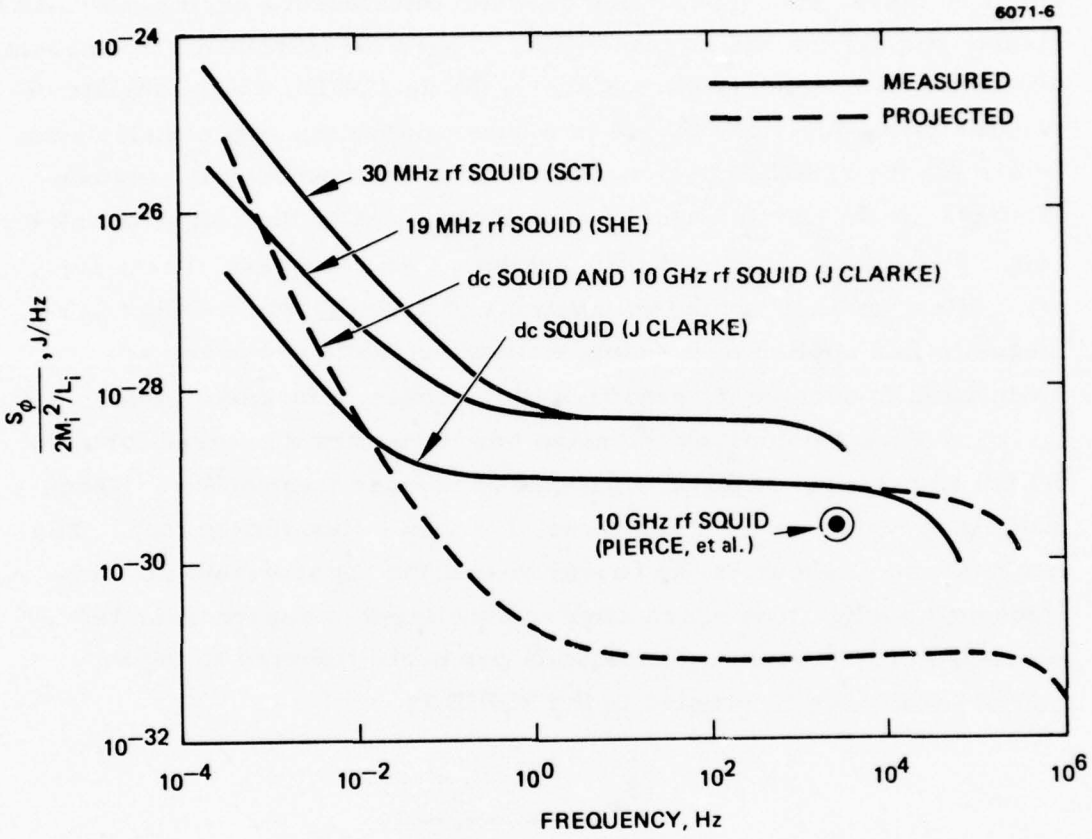

Figure 4.
Noise power spectra for SQUIDs operated in a flux-locked loop. The figure of merit shown is the energy resolution appropriate for low-frequency applications requiring transformer coupling.

$3.5 \times 10^{-5}\ \phi_o\ \mathrm{Hz}^{-1/2}$; (2) frequency response of 0 to 50 kHz; (3) dynamic range $\pm 3 \times 10^6$ or 135 dB in a bandwidth of 1 Hz; and (4) a slewing rate of $2.5 \times 10^5\ \phi_o\ \mathrm{s}^{-1}$. The slewing rate is defined as the rate $\omega\phi_f$ at which feedback flux changes. For a given slewing rate, an increase in frequency of the modulation flux, hence an increase in the SQUID frequency response, required a decrease in the amplitude of the feedback flux to avoid removing the flux-locked condition. Finally, by regulating the temperature of the helium bath to 50 μK, a long-term drift rate of $2 \times 10^{-5}\ \phi_o\ \mathrm{hr}^{-1}$ was achieved over a 20 hr period.

The sensitivity of the rf SQUID generally improves as the rf device frequency increases. Energy resolutions of 5×10^{-29} J Hz^{-1} and 2×10^{-30} J Hz^{-1} have been reported for SQUIDs operated with, respectively, 30 MHz and 10 GHz rf drive. Flux noise of $7 \times 10^{-6}\ \phi_o\ \mathrm{Hz}^{-1/2}$ has been achieved using a 440 MHz point contact SQUID. Values for other performance parameters are similar to those found for the dc SQUID: a dynamic range of $\pm 10^6$ in a 1 Hz bandwidth, a frequency response of 0 to a few kHz, and a slewing rate of 10^5 to $10^6\ \phi_o\ \mathrm{s}^{-1}$.

The intrinsic noise limit of these SQUIDs can be calculated from a detailed theory. Cruder physical arguments give resolution limits which agree with the theory (within a factor of 2 or 3). For example, assuming the intrinsic noise of the dc SQUID can be approximated by the Johnson noise in the resistive shunts, the energy resolution is

$$\frac{S_\phi}{2L} \approx \frac{2kT}{R/2L} \ ,$$

where T is the SQUID temperature and R is the shunt resistance of a single junction. Taking R = 1 Ω, L = 10^{-9} H, and T = 4K as typical values, $S_\phi/2L \approx 2 \times 10^{-31}$ J Hz^{-1}.

Jackel and Burman[47] have evaluated three sources of noise in the rf SQUID: intrinsic noise, tank circuit noise, and preamplifier noise. Assuming the preamplifier has a low enough noise temperature — a requirement difficult to satisfy at higher frequencies — the thermal noise generated by the tank circuit usually dominates the rf SQUID noise. The tank circuit noise $S_\phi^{(tc)}$ is found to be proportional to kT_e/ω, where ω is the resonant frequency and T_e is the effective temperature of the tank; for $T_e \approx 200$ K and $\omega = 30$ MHz, $S_\phi^{(tc)}/2L \approx 4 \times 10^{-30}$ J Hz^{-1} (Ref. 45).

The energy resolution of the dc SQUID may be improved by either increasing the junction resistance R or decreasing L, which most likely would decrease the coupling efficiency to the signal coil. Increasing R from 1 Ω to 100 Ω and letting L = 1 nH, the energy resolution per hertz approaches 10^{-32} J Hz^{-1}. An rf SQUID pumped at 10 GHz should obtain the same performance (assuming $T_e = 4$ K, R = 1000 Ω, and L = 1 nH).

Table 4 presents a summary of the performance of the SQUID sensor as a magnetometer, a magnetic-field gradiometer, and a voltmeter. These SQUID devices have found use in diverse applications, including submarine communications,[48] geophysics, and medical physics. As seen from Table 4, the SQUID is an extremely sensitive magnetometer. In many applications, magnetic signals are coupled into the SQUID using a superconducting flux transformer loop. The flux transformer contains two coils: (1) a loop of area A_2 and inductance L_2 coupled by mutual inductance $M_2 = \sigma (L L_2)^{1/2}$ to a SQUID operated in the feedback mode and (2) a pick-up coil of area A_1 and inductance L_1.

The optimum sensitivity of the system, found by equating the flux applied to the SQUID to the flux noise of the SQUID, $\alpha\Phi_o B^{1/2}$, and taking $L_1 = L_2$, is

$$\delta H = \frac{2\alpha\Phi_o (B L_1/L)^{1/2}}{\mu_o A_1 \sigma} ,$$

Table 4. Performance of SQUIDs in Low-Frequency Applications

Device	Ref.	Temp, K	Figure of Merit Measured	Frequency Range, Hz	Bandwidth, Hz	Dynamic Range, dB	Other Parameters
Magnetometer							
dc SQUID	44	4.2	$3.5 \times 10^{-5}\ \phi_o/\sqrt{Hz}$	(2×10^{-2}, 2,000)	1	140	Slew rate $2\times10^{4}\ \phi_o\ s^{-1}$
		4.2	$10^{-5}(1/f)^{1/2}\ \phi_o/\sqrt{Hz}$	$<2\times10^{-2}$	1	140	Drift rate $2\times10^{-5}\ \phi_o\ h^{-1}$
		1.8	$2\times10^{-5}\ \phi_o/\sqrt{Hz}$	(2×10^{-2}, 2,000)	1	140	over 20h period
		4.2	7×10^{-30} J/Hz	(2×10^{-2}, 2,000)	1	140	
		4.2	$\sim10^{-10}$ G/$\sqrt{Hz}$	(2×10^{-2}, 2,000)	1	140	
19 MHz rf SQUID	45	4.2	$7\times10^{-4}\ \phi_o/\sqrt{Hz}$	(10^{-2}, 5,000)	1	140	Slew rates 10^{5} to $10^{6}\ \phi_o\ s^{-1}$
	48		5×10^{-29} J/Hz	(10^{-2}, 5,000)	1	140	
30 MHz		4.2	$2.5\times10^{-5}\ \phi_o/\sqrt{Hz}$	(1, 1,000)	1	140	
			5×10^{-29} J/Hz	(1, 1,000)	1	140	
440 MHz	65	4.2	$7\times10^{-6}\ \phi_o/\sqrt{Hz}$	-	-	-	
10 GHz	46	4.2	$1\times10^{-5}\ \phi_o/\sqrt{Hz}$				
			2×10^{-30} J/Hz	>1,000			
Gradiometer							
rf SQUID	56	4.2	3×10^{-12} G/cm/$\sqrt{Hz}$				Balance against uniform field fluctuations: 1 part in 10^{7}
dc SQUID	51	4.2	2×10^{-10} G/cm/$\sqrt{Hz}$	(5×10^{-2}, 2,000)			1 part in 10^{4}
Voltmeter							
	52	4.2	4×10^{-13} V/$\sqrt{Hz}$		1	4×10^{4}	Source resistance $R_0 \sim 10^{-4}\ \Omega \leq 1\Omega$
	66	1	8×10^{-16} V/$\sqrt{Hz}$				Slewing rate 10^{-9} Vs^{-1} $\left[Vs^{-1}\right]$ $R_0 \sim 10^{-8}\ \Omega$
rf attenuation	67	4.2	10^{-9} W[a]	(dc, 10^{9})		62	

[a] Measurements of power at lower levels are accomplished with a narrow-band coupling circuit. Noise levels of 10^{-17} W have been found in the 100 MHz to 1 GHz frequency range.

where $\alpha\Phi_o$ is the flux resolution in a 1 Hz bandwidth and B is the operating bandwidth. To maximize this quantity, the effective volume of the pick-up coil is made as large as possible (i.e., A_1), and the loop length is increased.

Using this flux transfer arrangement, a magnetometer system achieved sensitivities of 2×10^{-11} G_{rms} $Hz^{1/2}$, limited by environmental noise rather than by intrinsic SQUID noise.[49] The measured magnetic field amplification factor between the pick-up coil and the SQUID was ~500.

Superconducting gradiometers measure the time-varying spatial derivatives of magnetic fields. The gradiometer consists of a SQUID coupled to a superconducting flux transformer which has two pick-up loops. These loops are balanced so that a change in a uniform field induces minimum supercurrent in the flux transformer. A gradient change does produce a supercurrent, which is detected by a flux-locked SQUID. The highest sensitivity reported for a gradiometer is 3×10^{-12} G cm^{-1} $Hz^{-1/2}$ (Ref. 50). This instrument has achieved balance against uniform field fluctuations and angular variations in position of one part in 10^7. A prototype thin-film, dc SQUID gradiometer, fabricated on a single planar substrate, has demonstrated sensitivities of 2×10^{-10} G cm^{-1} $Hz^{-1/2}$ and a balance of 1 part in 10^5 (Ref. 51). Increasing the loop size, improving the matching between loop and SQUID, and reducing the flux noise in the SQUID may improve the gradiometer sensitivity by one to two orders of magnitude.

For the measurement of small voltages, the SQUID is coupled by a mutual inductance $M = \sigma(L\ L_2)^{1/2}$ to a superconducting coil of inductance L_2 which is in series with a standard resistor R_s and the unknown voltage V_o. The voltage source resistance is R_o. Again using the SQUID in a flux-locked loop, it serves as a null sensor with current feedback to the standard resistor R_s. Among other advantages, the feedback enhances the input impedance of the voltmeter and decreases its response time.

Estimates of the noise temperature, T_N, find $T_N \simeq 10^{-6}$ K. Under conditions such that Johnson noise in R_o dominates SQUID noise, measurement of the noise in a 3 $\mu\Omega$ resistor down to a few millikelvin has been made.[52] The Johnson noise power in a resistor is 4 kTB, about 6×10^{-23} W at 1 K in a 1 Hz bandwidth. Measurements at this sensitivity level are made routinely, e.g., the rms noise voltage in a $10^{-8}\ \Omega$ resistor at 1 K, 8×10^{-16} V/Hz$^{1/2}$, is observable. The upper limit on the source resistance R_o is set by the largest coil inductance which can be coupled to the SQUID. In the system used by Giffard et al.,[52] this upper limit was $R_o \simeq 1\ \Omega$.

D. REVIEW OF CRYOGENIC REFRIGERATORS

Because the phenomenon of superconductivity is the basis for the Josephson effect, the devices and circuits built with JEDs must operate at temperatures below ~20 K. Therefore, some type of cryogenic support equipment must be included as part of any operating component. The intended use of the component will have a great deal of influence on the design of the cryogenic subsystem because there are many different ways to achieve the needed temperatures and cooling rates, and the various design choices can produce very different results in terms of size, weight, power consumption, reliability, and cost.

Most of the refrigeration schemes fall into two broad categories: passive and active. The passive systems are like the classical dewar in which a reservoir of cryogen (solid or liquid) stabilizes the temperature and provides the cooling power by going through a change of phase. In the active systems, there is generally some type of mechanical refrigerator which must be supplied with power constantly to maintain the desired low temperature of the circuit. Generally the passive systems can be very reliable, but they tend to be too large for applications which require long periods of unattended operation. The active types can be much more compact but are relatively inefficient (typically

0.1 to 1%) and have limited operating lifetimes. Airborne refrigerators have been demonstrated with lifetimes of 4000 hr producing temperatures of 77 K. Currently, there are programs underway at Hughes to substantially improve the reliability of the low-temperature (15 to 40 K) refrigerators. The goal is to obtain 20,000 hr operating lifetime.

We believe that the penalties involved in supplying cryogenic support to a receiver are not as great as would be encountered in increasing system performance in other ways. For example, in a typical system with an 8-dB-noise-figure receiver and a 20-W, 10%-efficient transmitter, the system margins could be improved by 5 dB by reducing the receiver noise figure to 3 dB or by increasing the transmitter power to 63 W. We have estimated that a closed-cycle refrigerator for such a receiver might consume ~100 W, weigh 5 lb, and occupy ~120 $in.^3$ In contrast, the increase in weight for just the power supply of the new transmitter would be ~65 lb, and the increased voltages and currents needed might cause reliability problems that are worse than those associated with the cooler.

That the reliability of cryogenic systems can be made consistent with the needs of military systems has been amply demonstrated. A wide variety of operating 77 K systems, both active and passive, are part of such systems as missile seekers and weapons guidance control systems. They have also been made part of IR sensor systems in satellites as well as in terrestrial applications. Because lower temperature cryogenic systems are still new to military applications, there is not a complete selection of refrigeration hardware available. However, development of improved refrigeration equipment is continuing, and the progress of those programs should be monitored to ensure that the proper hardware is available when it is needed by a JED subsystem.

To give a concise summary of current refrigeration capabilities, we include here a summary of the status of refrigeration equipment that was prepared by Bruno Leo of the Cryogenics and Thermal Controls Department in the Electro-Optical Division of Hughes.

1. Joule-Thomson System

The closed Joule-Thomson (J-T) system is well developed, but it has not been widely used because of its high power consumption and the possibility that the restricting orifice or J-T valve may become clogged. For cooling electronic devices, this system generally produces about 0.5 to 2 W of refrigeration at a temperature of 88 K or 77 K, depending on whether argon or nitrogen is used as the refrigerant.

Basically, a J-T system contains only two critical components: the compressor and the heat exchanger. Lubricated, dry, and diaphragm-type compressors have been built and used with this type of system. Lubricated compressors usually have the longest operating life; however, special provisions must be made to remove all traces of lubricant from the working fluid to prevent such contaminants from freezing out and plugging the system. Dry compressors employ solid lubricants, such as teflon. Because of the high pressure differences normally encountered between the stages of typical J-T compressors, the wear rates of dry lubricants are quite high and therefore the effective operating lifetime of the compressor is greatly reduced. In addition, these wear products must be removed from the gas stream to prevent plugging; however, much less filtering is needed than that required in oil-lubricated systems. As the name implies, diaphragm-type compressors depend on the flexing action of a diaphragm to compress the gas. The operating life of such a compressor has been quite limited because of the unavailability of a diaphragm material that is not subject to fatigue failure during continual cycling at moderately high pressure differentials. Ideally, no contaminants are introduced into the working fluid; however, in practice, it has been found that foreign materials, which we believe are introduced by the combination of diaphragm flexing and system outgassing, must still be eliminated from the gas stream. Much less filtering is required than that needed with either lubricated or dry compressors.

The use of efficient heat exchangers is essential to the construction of practical J-T systems as well as of all other closed-cycle cryogenic refrigerators. To obtain a reasonable process efficiency with such a system, the heat transfer surface areas must be large to keep temperature differences to a minimum. The pressure drop along the heat exchanger must also be kept to a minimum to maximize the J-T cooling possible when a minimum amount of power is applied to the system. The incorporation of a highly efficient heat exchanger in the design of a J-T refrigerator is extremely important in order that the cooling capacity and cooldown characteristics of the system may be optimized.

In addition to these general remarks concerning different types of compressors, the high gas pressures required for J-T cooling necessitate the use of high-speed machinery in order that the overall refrigerator volume may be kept to a minimum. Regardless of which type of compressor is used, it is apparent that the operational life will be quite limited unless a major advance is made in the present state of the art of compression-type machinery.

2. Claude System

This system is well developed; it can provide about 2 W of refrigeration at 2.5 K. By applying both the Claude liquid and gas cycles, temperatures ranging from 300 to 2.5 K can theoretically be achieved. Reciprocating engines or turbines are generally used to expand the gas; however, the use of turbines to cool loads of less than 20 W has not yet been demonstrated successfully. Helium is usually the refrigerant used in the Claude cycle.

To achieve practical machines, the mechanical expanders must operate reliably at low temperature, and only a minimum amount of gas should be allowed to leak past the piston. Reciprocating expanders have been built in which piston rings provide the seal between the piston and the cylinder and that employ very precisely machined pistons and cylinders to minimize gas leakage. Expanders using rings on the piston have a rather limited operational life because of wear on the

seal caused by sliding friction. Expanders that depend on a close fit between piston and cylinder generally have longer operating lives since they use the gas "blow-by" as a means of lubrication and are therefore subject to little or no wear. However, impurities in the gas stream sometimes cause the expander piston to seize in its cylinder, thereby rendering the refrigerator inoperative.

The use of reciprocating expanders also requires the incorporation of inlet and exhaust valves with their associated linkage and timing mechanisms. Here again, the problem of wear is encountered not only with the linkage mechanism but also with the valves and valve seats, which must be essentially leak-tight at low temperatures.

From the previous discussion, it is apparent that the use of reciprocating-type expanders entails a fairly complex mechanical arrangement. Machines of this type have been operated reliably for periods of more than 250 hr. Although we expect that this value can be increased, it is doubtful whether reliable operation for more than 1000 hr can be achieved within the foreseeable future.

The use of turbomachinery affords a means of achieving reliable operation for longer periods. If the reciprocating expander were to be replaced with a turbine expander, the identical operation would be performed in a somewhat different manner. Cooling could result since some of the energy within the gas would be converted into work by the turbo-expander. However, since it is a continuous-flow machine, the turbine would not require valves. Turbine-type devices lend themselves to the use of gas bearings; if these are properly designed, such devices can operate many thousands of hours with little or no wear or contamination. Also, for an equivalent size, a turbine can handle much larger volumes of gas per unit time and thereby allow the generation of a greater amount of refrigeration.

3. Stirling System

The Stirling system reached its greatest development after 1947; the performance of a system based on this cycle agrees fairly well with

that predicted by theory. Systems of this kind can produce refrigeration ranging from milliwatts to kilowatts, usually over a temperature range of from 300 K to 30 K. Helium is generally the working fluid used, and a decrease in temperature from 300Kto 70 K has been obtained and maintained by using a Stirling-cycle refrigerator having a one-stage expansion cyclinder. Units weighing approximately 15 to 20 lb have been operated for long periods of time and have provided about 10 to 15 W of refrigeration at 77 K.

Practical machines based on this cycle have a compression volume at the higher-temperature end (room temperature) and an expansion volume at the lower-temperature end, which is in direct contact with the cold end. A regenerator between these two volumes serves alternately as a heat sink and a heat source. A Stirling machine requires no valves because the gas charge is cycled through the system by the out-of-phase motion of two pistons that are either in one cylinder or in two separate cylinders. These pistons are driven by a crank that provides this out-of-phase motion. Piston rings made of teflon-filled material are generally used to keep gas "blow-by" to a minimum. The surfaces of the bearings in the drive mechanism are typically dry lubricated or lubricated with grease having a low vapor pressure.

The regenerator is the heart of a Stirling-cycle refrigerator. Its design largely influences the ultimate temperature at the cold end as well as the refrigeration capacity that can be achieved. Typically, it consists of an assembly of metal plates, wire gauze, or fine metal shot arranged in such a way that large surface areas are exposed to the flow of gas to ensure maximum heat transfer.

Special care must be taken to prevent the "channeling" of the gas flow (unequal distribution of the flow through the regenerator packing) and to keep resistance to the flow of gas to a minimum. Since the regenerator is a single-fluid heat exchanger that alternately absorbs and releases heat, its performance depends to a large extent on the thermal capacity of the packing material. Below 100 K, the specific heat of all solids decreases rapidly with decreasing temperature, and it eventually reaches a point at which the therml capacity of the working fluid becomes considerably greater than that of the metals used in

the regenerator. There are some materials (for example, lead) that retain a useful thermal capacity down to temperatures of 10 to 20 K.

Helium gas is typically the working fluid used since it causes no phase-change problems in the system. This is an important consideration since the Stirling cycle depends on the continuous compression and expansion of the working fluid to provide the refrigeration.

In general, the wear associated with bearing surfaces and seals in Stirling-cycle machines is much less than that typical of J-T refrigerators since in Stirling systems the pressure ratios as well as the operating speeds are relativly low (typically 1200 rpm). In practice, Stirling-cycle refrigerators are also quite tolerant of contaminants. This behavior can best be explained by examining the pattern in which the gas flows through the regenerator. The regenerator, because of its narrow passages, is the system component that is most likely to become plugged. If contaminants do become "frozen out" within the regenerator matrix, the continual reversal of the gas flow has the tendency to flush them away and thereby provide a self-cleaning action. This is in direct contrast to a unidirectional system, such as a J-T cooler, where the contaminants continue to build up until complete plugging results.

A maintenance-free life of 500 hr has been achieved at Hughes with Stirling-cycle coolers; this can be increased with further development.

4. Gifford-McMahon or Ericsson System

This system is fairly well developed. Systems with three stages have been built in which the first, second, and third stages have a refrigeration power of 1000, 225, and 200 mW, respectively. The corresponding temperature limits are 100, 45, and 4 K. In these systems, helium is also the working fluid used.

This type of machine has several important advantages. As with the Stirling-cycle machine, its mechanical construction is relatively simple. For instance, it requires no close-tolerance rubbing parts in the low-temperature zone. It uses only one seal per displacer and only two valves, regardless of the number of displacers. Since both

the displacer seals and the valves are in a room-temperature location, they can be made of elastomeric materials. Another desirable feature is the ease with which additional stages can be added to reach lower temperatures. For example, a second stage can be incorporated by providing an additional regenerator in series with the first, and another displacer with the cold volume at the bottom of the second regenerator and with a common warm volume for the two displacers. The heat from the second displacer is pumped through the first regenerator and dissipated at room temperature. Another important feature is that the highest efficiency is realized when the displacers are operated at a low speed, e.g., from 50 to 100 rpm. Since at such speeds there is less vibration and fatigue as well as less wear on the working parts, there is the potential for longer operating life.

In contrast to the conventional Stirling-cycle machine, one of the penalties associated with the Gifford-McMahon machine is an inherently small decrease in cycle efficiency. Also, in addition to requiring two valves (whereas the Stirling-cycle refrigerator uses no valves), this type of refrigeration also requires a separate motor and crosshead mechanism to drive the displacers. Although not much power is needed to move these displacers, the additional drive mechanism increases the mechanical complexity of the refrigerator and could influence its overall reliability.

5. Solvay System

The Solvay system has reached a fair stage of development. One model based on this cycle is a cascaded, two-stage machine that can provide 1 W of refrigeration at 16 K. Another model is a three-stage system in which a J-T cycle is used for the last expansion. The refrigeration available at the first, second, and third stages is 15, 9, and 1.5 W, respectively. The corresponding temperature limits are 150, 50, and 15 K. The Solvay refrigerator is located some distance from the compressor. Unlike the Gifford-McMahon system, the Solvay system operates on a work-producing cycle. In this respect, it is

similar to a reciprocating Claude-cycle system; however, the way in which it is used during the refrigeration cycle more nearly approximates the operation of a Stirling-cycle machine. As in the other modified Stirling-cycle machines, the remotely located comprssor can be either dry or lubricated by oil. One of the advantages of this machine is that it can be packaged in a relatively small volume. The length of its maintenance-free life depends to a large extent on the performance of the seals and of the compressor package.

6. Vuilleumier System

The development of this system, which is related to the Stirling system, has progressed steadily since Hughes built its first Vuilleumier (VM) unit in 1967; since then, several units have been used in Army, Navy, and Air Force projects. Unlike the other systems previously discussed, the VM system operates with very low pressure differentials across its pistons. The only purpose of the pistons is to secure the regenerators and to move the helium refrigerant alternately from the hot to the cold ends. Thus, the pressure differentials across the seals are due only to dynamic drag of the refrigerant and not to compression. In addition, a VM refrigerator runs at low speeds (less than 1000 rpm) and its operation is very quiet. This type of refrigerator is therefore potentially capable of a maintenance-free operating life that is appreciably longer than any that has yet been achieved. It can be driven by any type of thermal power, such as electrical, solar, combustible fuel (liquid or solid), or radioisotopes.

The electrically powered VM system used in the CMP space program operated 500 hr in space, and an identical model of this system logged 2200 hr of operation without the need for maintenance during tests at the Hughes Ground Systems Group facility in Fullerton, California. In 1973, the VM refrigerator that Hughes tested for the Honeywell Radiation Center accumulated a maintenance-free operating time of 3586 hr. VM systems are generally capable of providing up to 5 W of refrigeration.

7. Reversed Brayton Systems

Both the rotary reciprocating and the turbine type of refrigerators suitable for use with infrared systems are still in their early stages of development. A rotary reciprocating expander that can provide 2 W of refrigeration at 77 K has been built and operated as part of a complete closed-loop refrigeration system. The most critical mechanical elements are the expansion engines and the system used to drive them. The factors having the greatest bearing on operational life are the life of the power conditioning equipment and the sensitivity of the bearings and seals to contamination.

8. Solid-Cryogen System

Several prototype or laboratory solid-cryogen systems have been built; the cryogens used include nitrogen, argon, CO_2, neon, methane, oxygen, and hydrogen. The Aerojet-General Corporation has built a refrigerator that employs solid nitrogen and is designed to provide 0.75 W of refrigeration for about 1000 hr. Lockheed constructed a 50 K argon-125 K CO_2 refrigerator capable of providing 25 mW of refrigeration for one year in space. The Ball Brothers Research Corporation built a similar refrigerator with a design goal of 14 mW of refrigeration at 77 K for one year.

All of these units were subject to thermal losses and their design goals were not reached. It is difficult to achieve good thermal coupling between the thermal rod and cryogen because of the sublimation that occurs at this interface. When the system is in the standby mode, power must be applied to the vacuum pump almost continuously to remove gas because of thermal losses. Because they are explosive, methane and hydrogen require special handling.

SECTION 3

NAVAL SYSTEM SURVEY

The survey of Naval systems for this program was performed in two parts. In the first part, the broadest possible view was taken, and a very large list of systems used in surveillance and communications was compiled. A classification scheme was developed to give order to the information accumulated. By using both technical data and data concerning the potential importance of the system to the Navy, a smaller list of systems was compiled which was representative of the wide variety of Navy needs and which was representative of the more advanced technologies being used in military hardware. In the second part of the survey, we collected more detailed information about the systems' configuration and performance. This information provided the basis for the recommendations made in Section 4.

A. SURVEY OF NAVAL SYSTEMS

The information for this part of the survey was gathered from a wide variety of sources. These included a selection of system and component designers who work in the Ground Systems Group, the Electro-Optical and Data Systems Group, and the Radar Systems Group of Hughes Aircraft Company. The Hughes personnel who served as consultants on this program have experience in many aspects of radar, communications, and electromagnetic surveillance and countermeasures systems. Table 5 contains a list of these consultants and their areas of expertise. In addition to these sources, data was collected from trade publications and from various Navy sources.

Under a subcontract from Hughes, Decisions and Designs, Inc., collected preliminary data on many of the systems and provided a list of contact points in the Navy from which more detailed information could be obtained. Table 6 contains a partial list of Navy personnel who contributed data to this study. In addition, information was

Table 5. Hughes Consultants for Naval System Survey

Consultant	Area of Expertise
W. H. Brackmann, Jr.	Sonar and ASW Systems
L. F. Brajkovich	Communication and Radar Systems
D. J. Braverman	Communication Satellites
W. P. Clark	Shipboard Radar Systems
R. D. Doody	Cryogenic Refrigeration Systems
V. H. Estrick	Microwave Receivers
D. G. Fawcett	Microwave Receivers
P. R. Hart	Digital Processing
S. C. Iglehart	Airborne Radar Systems
G. Kemanis	Communication Satellites
W. K. Masenten	Radio Receivers
R. L. McGhie	ECM Systems
A. Mellas	Shipboard Radar Systems
G. C. Rosholt	ECM Systems
W. H. Walters	Communication Systems
F. C. Williams	Radar Systems

Table 6. U.S. Navy Information Sources

R. O. Eastman	NELC
J. Grant	Strategic Systems Project Office
H. C. Kung	NAVELEX
M. Nisenoff	NRL
J. J. Schwartz	NAVELEX
D. H. Townsend	NRL
C. J. Waylan	NAVELEX
H. Whitehouse	NUC
D. O. Wilson	NAVELEX

collected from people in the following organizations: ONR, NELC, NAVELEX, NRL, NADC, NAVAIR, PM-1 (Strategic Systems Project Office), PM-2 (Trident Systems Project Office), and DDR&E.

To organize this information in a useful way, a classification system with three dimensions was developed. This classification system is shown schematically in Figure 5. The identified systems were evaluated according to this classification scheme, and they are listed in Table 7. From this list, systems were chosen to represent the complete spectrum of Naval needs. In choosing the systems, first consideration was given to those that utilize the most current technology and to those that are more widely deployed, so that potential costs and benefits would be significant.

The list of systems that were chosen for the more detailed analysis is shown in Table 8 together with a display of the way that they fit in the classification scheme. Clearly, not all combinations are covered, but those which are not covered are not generally of great interest to the Navy. One exception to this is the low-frequency (ELF) communication application. A specific piece of equipment was not identified for this application, but the applicability of Josephson-effect devices to this and to the VLF communication areas is discussed in Section 4.

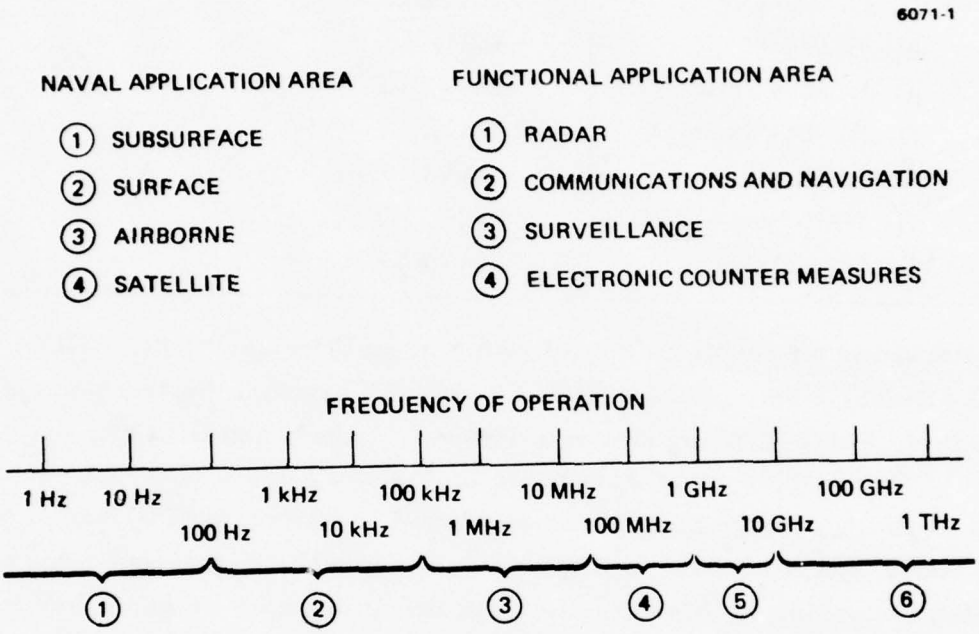

Figure 5. Description of system classification scheme.

Table 7. Classification of Naval Systems

System	Naval Application				Functional Application				Frequency					
	1	2	3	4	1	2	3	4	1	2	3	4	5	6
AN/BPS-13 Periscope radar	X				X								X	
AN/BPS-15 Surface Search	X				X								X	
AN/AWG-9 Fire Control (F-14)			X		X								X	
AN/SPN-35 Landing Control		X			X								X	
AN/SPN-41 Landing Control		X	X		X									X
AN/SPN-42 Landing Control		X			X									X
AN/SPN-43 Air Traffic Control		X			X								X	
AN/SPN-44 Aircraft Speed Detector		X			X									X
AN/SPS-5D Surface Search		X			X								X	
AN/SPS-30 Air Search		X			X								X	
AN/SPS-32/33A Air Search		X			X							X	X	
AN/SPS-37A Air Search		X			X							X		
AN/SPS-39A Air Search		X			X								X	
AN/SPS-40 Air Search		X			X							X		
AN/SPS-43 Air Search		X			X							X		
AN/SPS-48 Air Search		X			X								X	
AN/SPS-49 High Resolution Air Search		X			X							X		
AN/SPS-52B 3D Air Search		X			X								X	
AN/SPS-53 Surface Search		X			X								X	
AN/SPS-55 Surface Search		X			X								X	
AN/SPS-57 Surface Search		X			X								X	
AN/SPY-1 Anti-Missile		X			X									
IPD/TAS Improved Point Defense		X			X								X	
AN/ALR-52 IFM and DF Receiver			X			X	X					X	X	X
AN/ARC-181 *JTIDS* Terminal			X			X							X	
AN/ARQ-40 JTIDS Terminal		X	X			X								
AN/BRD-7 RDF Set	X					X	X					X		
AN/BRN-38 Satellite Navigation Receiver	X					X					X			
AN/BRR-3 VLF Communications	X					X				X				
AN/GRC-112 FM Transceiver		X				X						X		
AN/PRC-41 AM SSB Transceiver		X				X						X		
AN/PRC-104 Portable Communications		X				X					X			
AN/SMQ-6 Metsat Receiver		X				X								
AN/SPN-32 Loran Receiver		X				X				X				
AN/SPN-38 Loran Receiver		X				X				X				
AN/SRC-20 SSB Transceiver		X				X						X		
AN/SRC-21 SSB Transceiver		X				X						X		
AN/SRC-23 NTDS Transceiver		X				X					X			
AN/SRC-31 NTDS Link 4		X				X						X		
AN/SRC-34 SSB Transceiver		X				X						X		
AN/SRN-12 Omega Receiver		X				X				X				
AN/SRN-17 Omega Receiver		X				X				X				
AN/SRR-1 SATCOM Receiver		X				X						X		
AN/SRR-13 General Purpose Receiver		X				X					X			
AN/SRR-19 Multi-Channel Receiver		X				X				X				
AN/SSC-3/6 SHF SATCOM Transceiver		X				X							X	
AN/UPN-15 Loran Receiver		X				X				X				
AN/URC-9 General Purpose Transceiver		X				X						X		
AN/URC-35 General Purpose Transceiver		X				X					X			
AN/URC-82 UHF Radio		X				X						X		
AN/URD-4 DF Set		X				X						X		
AN/URD-7 Special DF System		X				X						X		
AN/URN-20 Tacan Receiver		X				X							X	
AN/URR-27 *Superhet Receiver*		X				X						X		
AN/WPN-3A Loran Receiver	X					X				X				
AN/WPN-4 Loran Receiver		X				X				X				
AN/WPN-5 Loran Receiver	X					X				X				
AN/WRC-1 SSB Transceiver	X	X				X					X			
AN/WRN-3 Omega Receiver		X				X				X				
AN/WRR-3 Shipboard Receiver	X					X				X	X			
AN/WRR-7 VLF Receiver	X					X				X				
AN/WSC-1/5 SATCOM Terminal		X				X						X		
AN/WSC-2 SHF SATCOM Terminal		X				X							X	
AN/WSC-3 UHF SATCOM Terminal		X				X						X		
AN/ALR-47 ECM Receiving Set			X				X	X						
AN/ASQ-81 MAD Set			X				X		X					
AN/BQQ-5 Sonar Set	X						X		X	X				
AN/BQR-15 Sonar Set	X						X		X	X				
AN/WLR-6 ELINT Receiver	X						X				X	X	X	X
AN/WLR-8 ESM Receiver	X	X					X			X	X	X	X	X
AN/ALQ-61 Passive ECM			X				X	X			X	X	X	X
AN/ALQ-91 ECM Set			X					X						
AN/ALQ-99(ALR-42)			X				X	X				X	X	X
AN/ALQ-100/126 ECM System			X					X					X	X
AN/ALQ-108 IFF Receiver			X					X						
AN/ALR-45 Radar Warning Receiver			X				X	X					X	X
AN/ALR-50 Warning Receiver			X					X						
AN/ALR-66 Radar Warning Receiver			X					X					X	X
AN/ALR-67 Radar Warning Receiver			X				X	X						
AN/BLR-10 ECM Receiver	X						X	X					X	
AN/SLQ-17A ECM System		X						X					X	X
AN/SLQ-31 EW System		X					X	X				X	X	X
AN/SLQ-32 *EW System*		X					X	X				X	X	X
AN/SLR-12 ECM Receiver		X						X						X
AN/WLR-1 Super Heterodyne Receiver	X	X					X	X				X	X	
AN/WLR-3 ECM Receiver		X						X						
AN/WLR-10 ECM Receiver		X						X					X	
AN/WLR-11 IFM Receiver	X	X					X	X					X	X
MARISAT Communication Satellite				X		X						X		
Sea Nymph ELINT	X						X				X	X	X	X

Table 8. Initial List of Systems Selected for Performance Tradeoff Study

System	Naval Application				Functional Application				Frequency					
	1	2	3	4	1	2	3	4	1	2	3	4	5	6
ALQ-100/126 ECM System			X					X					X	X
ALQ-99(ALR-42) EW System			X				X	X				X	X	X
ALR-66 Radar Warning Receiver			X					X					X	X
ARC-181 JTIDS Terminal			X			X							X	
ASQ-81 MAD			X				X		X					
AWG-9 Fire Control (F-14)			X		X								X	
BLR-10 ECM Receiver	X						X	X					X	
BPS-15 Surface Search	X				X								X	
BQQ-5 Sonar Set	X						X		X	X				
BRN-38 Satellite Navigation Receiver	X					X					X			
BRR-3 VLF Communications	X					X				X				
SLQ-17A ECM System		X						X					X	X
SCQ-31 EW System		X					X	X				X	X	X
SPS-52B 3D Air Search		X			X								X	
SPN-35 Landing Control		X			X								X	
SPN-42 Landing Control		X	X		X									X
SRR-1 SATCOM Receiver		X				X						X		
WLR-6 ELINT Receiver	X						X				X	X	X	X
WLR-8 ESM Receiver	X	X					X				X	X	X	X
WPN-5 ESM Receiver	X					X				X				
WRR-3 Shipboard Receiver	X					X				X	X			
WRR-7 VLF Receiver	X					X				X				
WSC-2 SHF SATCOM Terminal		X				X							X	
WSC-3 UHF SATCOM Terminal		X				X							X	
MARISAT Communication Satellite				X		X						X		

B. SUMMARY OF SYSTEM CHARACTERISTICS

To keep this report unclassified and to maintain the organization of this section, the detailed system characteristics have been published as a classified Addendum entitled "Addendum to Systematic Survey of Naval Surveillance and Communications Systems: Summary of Operating System Characteristics (U)" (Contract N00173-76-C-0389, SDN P-58593).

Table 9. Final List of Systems Surveyed for the Study

AN/ARC-181	JTIDS Compatible Terminal
AN/ASQ-81	Magnetic Anomaly Detection Set
AN/AWG-9	F-14 Fire Control Radar
AN/BLR-10	Countermeasures Receiving Set
AN/BPS-15	Submarine Surface Search Radar
AN/BQQ-5	Sonar System
AN/SLQ-17A	Aircraft Carrier ECM System
AN/SLQ-31	Design-to-Price EW Set
AN/SPS-52B	3-D Air Search Radar
AN/SSR-1	SATCOM Fleet Broadcast Receiver
AN/WLR-6	ELINT Receiver
AN/WLR-8	ESM Receiver
AN/WRR-7	Submarine VLF Broadcast Receiver
AN/WSC-2	SHF Satellite Communication Transceiver
AN/WSC-3	SATCOM Shipboard Transceiver
MARISAT	Communication Satellite

SECTION 4

ANALYSIS OF FUTURE APPLICATIONS FOR JEDs

A. RECEIVER APPLICATIONS

1. Effect of Receiver Sensitivity on System Performance

Communication and surveillance systems must perform a function in which they detect radiation in the surrounding environment. In communication systems, there is a distant transmitter which generates the signal. In radar, the signal results from the scattering of the system's own transmission. In ECM and surveillance systems, a hostile source is generally the originator of the signal. In each system there is generally a trade-off between various aspects of system performance and the receiver's sensitivity. For example, the size and weight of the system, the operating range, and the error rate are all parameters which could be affected by the receiver sensitivity, i.e., the level of noise generated in the receiver.

A very general way to assess the effect of receiver sensitivity on a system is to compare the noise generated by the receiver with the noise that is collected, along with the desired signal, by the system's antenna. Thus, one can find the ratio between the receiver noise power, P_R, and the noise power collected by the antenna, P_A. It is more usual to express the power in terms of an effective temperature through the expression

$$P = kTB,$$

where k is the Boltzmann constant, B is the noise bandwidth of the system, and T is the effective noise temperature. Thus, we can discuss the system in terms of its antenna temperature, T_A, and the receiver temperature, T_R. In cases where the receiver sensitivity is given in

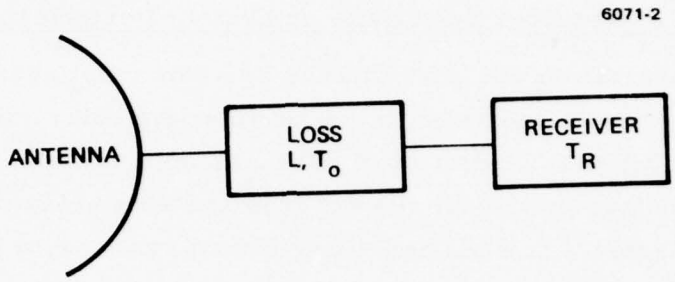

Figure 6. Basic receiver configuration.

terms of noise figure, F, we can find the equivalent noise temperature using $T = (F - 1)\ 290$ K.

In addition to antenna noise and receiver noise, system front-end noise is also generated by the losses between the antenna and the receiver. These losses can be caused by cable or waveguide runs, multiplexers, duplexers, rotary joints, filters, switches, or other types of circuitry. These losses can be associated with a noise temperature at the output of the element

$$T_L = \left(1 - \frac{1}{L}\right) T_o ,$$

where L is the reciprocal of the gain associated with the lossy element and T_o is the physical temperature of the lossy element.

A typical system front-end can be represented by the diagram in Figure 6. If we calculate the total system noise at the antenna, we find

$$T_S = T_A + (L - 1)\ T_o + L\ T_R .$$

The system can have a favorable tradeoff with improved receiver sensitivity (i.e., reduced T_R) so long as

$$T_R > a\left[\frac{T_A}{L} + \left(1 - \frac{1}{L}\right) T_o\right],$$

where a is an arbitrary factor close to 1. Thus, there are two factors which define a minimum practical receiver noise temperature, T_{min}, for a system: the antenna noise and the added noise due to front-end losses.

In Figure 7 we show how these two noise contributions interact to define T_{min} (a is taken to be 0.5). One curve is plotted for the system

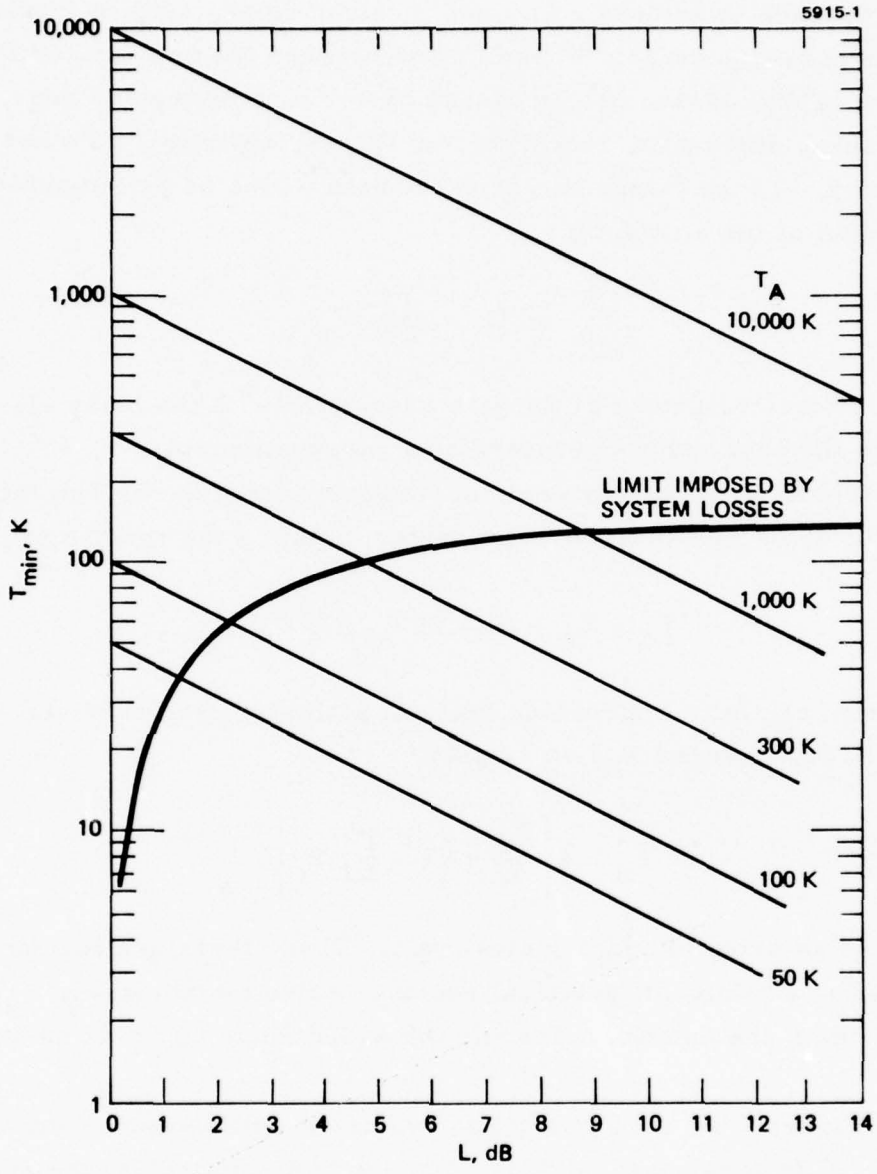

Figure 7. Receiver noise limits resulting from environmental noise and front-end losses.

losses with T_o assumed to be 300 K. A family of curves is plotted for the antenna noise contribution. Naturally, this contribution depends on the value of the antenna noise, T_A. In Figure 8, we show typical behavior for the antenna temperature as a function of the frequency. This noise has three sources. One source is the electrical activity in the sun and other stars. Another is the attenuation in the atmosphere. The last is the man-made machinery and other electrical systems. The level of antenna noise experienced by any particular system will depend on the antenna beamwidth, the direction it points, and the location of the system. The noise level is generally lowest when the antenna points up into the sky. For example, antenna noise for typical satellite communication links is 300 K in X band and 1000 K in UHF. At frequencies lower than UHF, atmospheric systems have quite high antenna temperatures.

2. Applications for Improved Receiver Sensitivity

Using the curves in Figures 7 and 8 together with the receiver performance information in Figure 9, we can delineate a subset of applications which operate in the atmosphere and which are good candidates for a potential receiver upgrade. From these charts we can see that, for systems operating below ~8 GHz, antenna noise is so high or current performance is so good that current receiver technology is adequate. However, systems above ~8 GHz can have antenna temperatures of 300 K or less. If we assume a minimum room temperature loss of 1.5 dB for a practical system, then the smallest practical T_{min} would be 80 to 200 K depending on the antenna noise.

In the 8 to 15 GHz region, state-of-the-art parametric amplifiers can achieve 120 to 150 K noise temperatures over moderate bandwidths of 20% or less. These bandwidths are typical of those used in most communication and radar applications. Thus, conventional technology would seem to be capable of satisfying the needs of most of these applications at frequencies below 15 GHz.

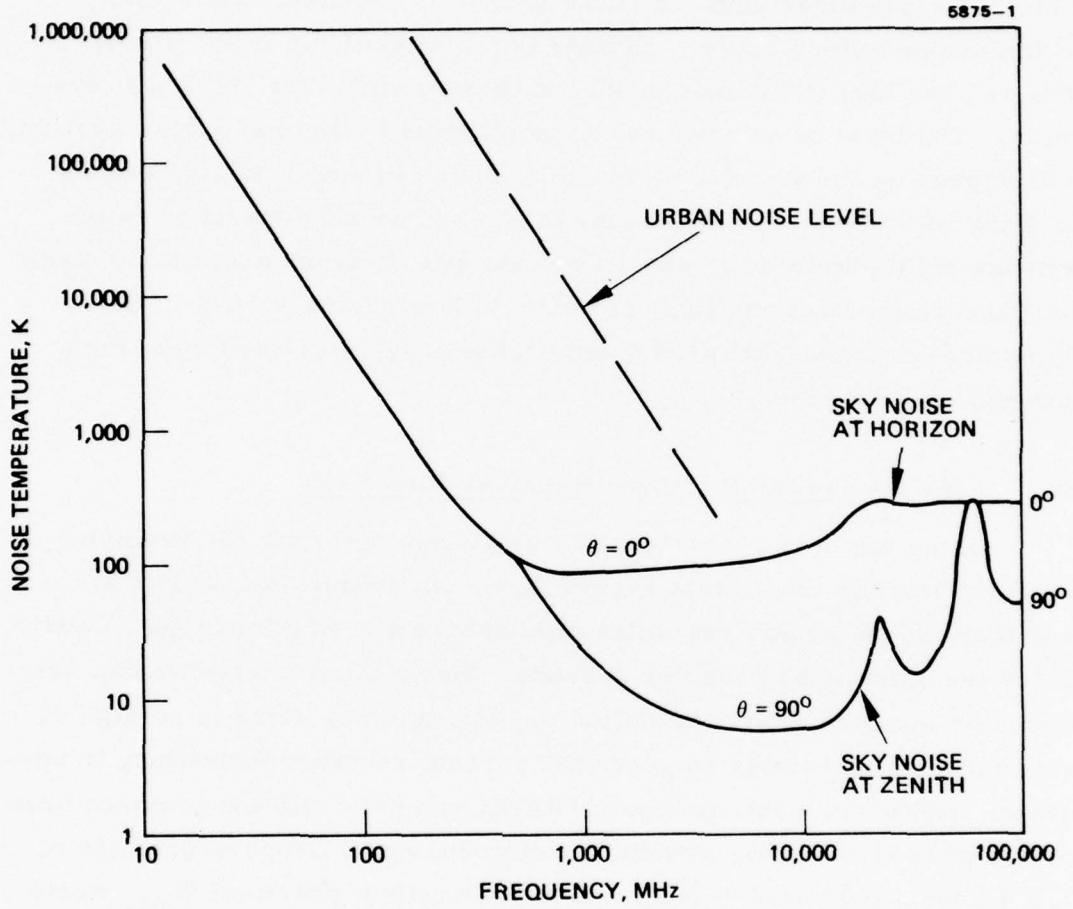

Figure 8. Atmospheric environmental noise.

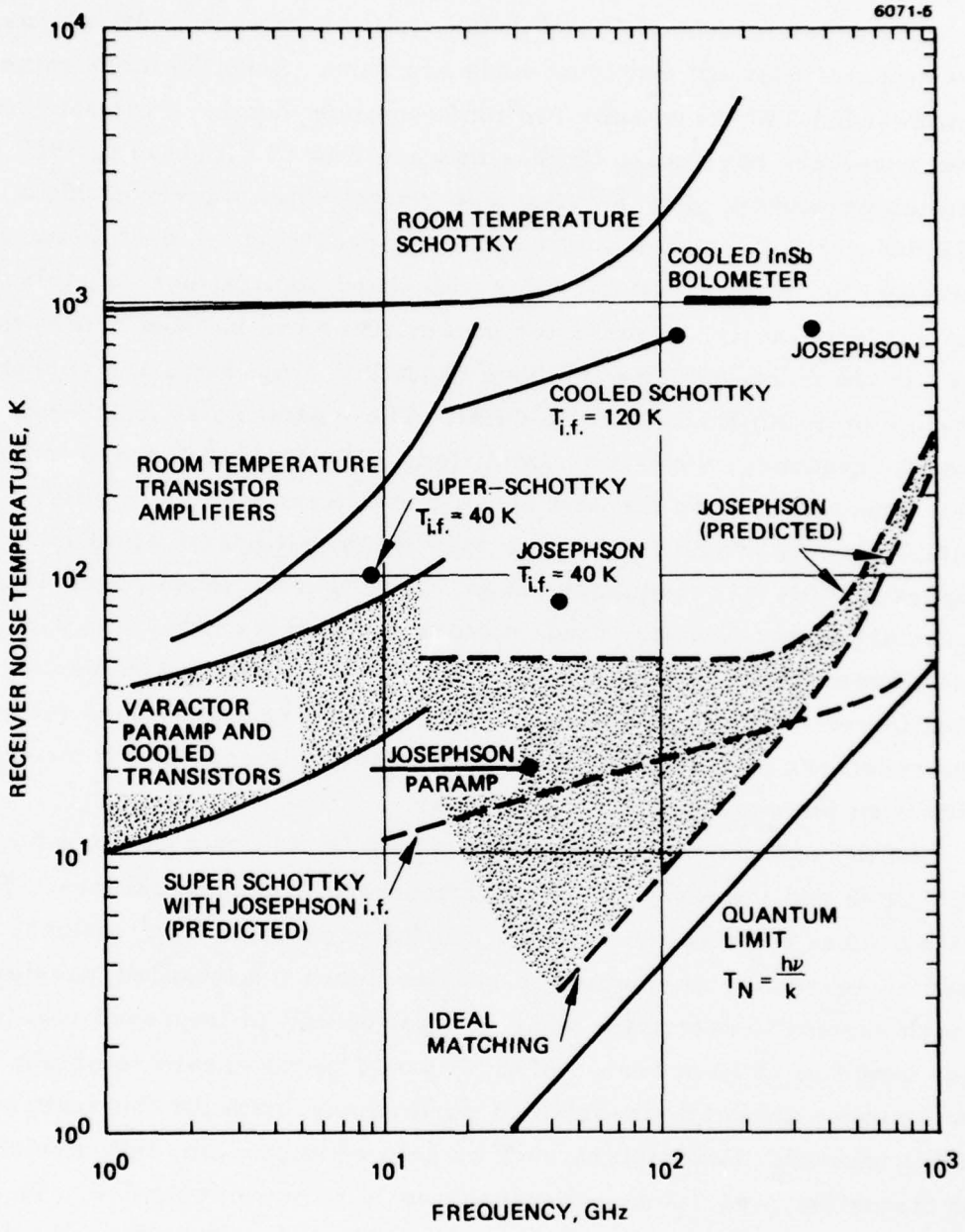

Figure 9. Low-noise receiver technologies.

For wider microwave bandwidths, i.e., octave or multi-octave, three types of conventional front-ends are used. Schottky diode mixers and wide-band TWTAs are the two most common types. Typically, the mixer receivers have noise figures that are 8 to 15 dB (1540 to 8900 K noise temperature). The TWTAs have typical noise figures of 12 to 20 dB and are only used in applications not requiring the best sensitivity (typically, the ECM systems). For wide-band applications requiring the utmost in sensitivity, a transistor preamplifier can be used before the mixer in the front-end. Such octave bandwidth amplifiers are currently available up to Ku band (12 to 18 GHz). The typical noise figure for the high-frequency, wide-band amplifiers is 7 dB (1160 K noise temperature). Therefore, even the best conventional technology currently available cannot provide receivers with the lowest practical noise temperature for this frequency range. As Figure 9 shows, both JED mixers and super-Schottky diode mixers can provide receivers with noise temperatures less than 300 K from low microwave frequencies up to millimeter-wave frequencies. Thus, low-noise, wide-band microwave receivers in surveillance equipment are a potentially promising application for superconductive devices.

Of the systems surveyed, those which fit this category are the AN/WLR-8 and the AN/WLR-6, both countermeasure receivers. To obtain a more definite conclusion about these potential applications, it would be necessary to examine in greater detail the intended mission of each system to determine what the real benefit of improved receiver noise would be in each case. Also, it would be necessary to obtain data on more applications-oriented performance data for the superconductive mixers. Parameters such as gain compression, intermodulation distortion, and damage threshold would be very desirable. To predict the properties of a well-integrated subsystem, more data should be generated on the characteristics of tunable JED oscillators.

As frequencies rise into the millimeter-wave region (30 to 300 GHz), the noise temperature of available receivers rises significantly. Because of the difficulties involved in generating sufficient high-frequency

pump power for parametric amplifiers, most receivers use Schottky diode mixers in the front-end. Thus, for communication and radar applications as well as for surveillance, typical receiver noise temperatures are 1000 to 10,000 K. Since antenna noise is generally below 300 K in the millimeter-wave portion of the spectrum and the general activity level is low (resulting in lower interference from other sources), the potential for improved system performance in this part of the spectrum is great. Section 3 showed that very few systems are currently operating at these frequencies. Nevertheless, it is generally felt that there is a trend toward increased utilization of the millimeter-wave bands, and there are many experimental systems exploring the use of that part of the spectrum for secure communications, high-resolution radars, and missile and RPV guidance.

As an example of the potential for superconducting device receivers in the millimeter-wave region, we consider an experimental 94 GHz radar that is being developed for DARPA and the Air Force by Hughes.[7] The mission for this radar is to obtain image data of strategic targets from a ground base. To operate at useful ranges, the system requires both transmitter and receiver performances that are beyond the present state of the art. Development work is currently being conducted on the component with the highest technical risk, the high-power transmitter. The receiver in this system performs a complex pulse compression function. Currently, its noise figure is 11.5 dB. If the transmitter development achieves its present goals, this system will require the development of a receiver with 3 to 5 dB noise figure. Both the super-Schottky mixer and the Josephson-junction mixer have excellent potential for this application. If sufficiently small devices can be made to achieve the kind of performance seen by Richards and his co-workers at 35 GHz, then a Josephson-junction mixer could yield a receiver noise temperature less than 200 K (2.3 dB noise figure) even using the current system i.f. amplifier, which has a 120 K noise temperature. If we similarly scale the super-Schottky performance seen at

9 GHz by Silver and his co-workers, we find that a 50 K i.f. amplifier is needed to provide a 300 K receiver.

The optimal approach to such a receiver is to provide an integrated unit that contains at least the mixer and the first stages of i.f. amplification. In some cases it may also be desirable and feasible to include the local oscillator source along with the mixer and amplifier; however, in coherent radar systems like this one, the local oscillator and other signals used in the radar must be phase locked to a single, stable reference frequency. Thus, for this application the mixer/amplifier unit is probably optimal.

The remaining applications for which superconductive device receivers offer potential improvements are at the low end of the frequency spectrum. As shown in Figure 7, low-noise receivers do not offer significant advantages in low-frequency atmospheric applications because the environmental noise level is very high. However, with submarine systems that receive radio signals below the surface of the ocean, the ambient atmospheric noise is attenuated by the lossy salt water medium. Both signal and noise are attenuated as a function of the distance from the surface so that the signal-to-noise ratio remains constant until the signal level approaches the thermal noise level. The characteristic attenuation depth is given by

$$\delta = \sqrt{\frac{4}{\pi f \sigma \mu}} \ ,$$

where f is the frequency, σ is the conductivity of the water (typically 4 mohs/m), and μ is $4\pi \times 10^{-7}$ in mks units. It is more useful to express δ in terms of an attenuation rate

$$\alpha = \frac{4.34}{\delta} \text{ dB/m} .$$

For frequencies of 44 Hz and 10 kHz (typical ELF and VLF frequencies), the attenuation rates are 0.23 dB/m and 3.5 dB/m, respectively. The practical limit on the depth will depend on the radiated power level available at the surface. The situation for two hypothetical cases is shown in Figure 10. For VLF the available S/N becomes less than one between 20 and 30 m. For the ELF example, reception is still possible down to 200 m.

Reception of these signals depends on both the receiver and the antenna. For an antenna that is matched to the propagating signal, a receiver with 1.8 to 3.0 dB noise figure will yield near-optimal system performance. This noise level is significantly below the performance level of the more advanced VLF receivers, e.g., the AN/WRR-7. Thus, if the current system is not dominated by the antenna-generated noise, improved receiver sensitivity would certainly be useful. If conventional devices are unable to provide the improved performance (possibly because the antenna impedances are very low), then the device study has shown that JEDs can make very sensitive amplifiers at these low frequencies, especially at low impedance levels. For example, the SQUID voltmeter has shown a noise temperature of ~100 K.

Because of their low impedance levels and exceptionally low noise levels, the SQUID amplifiers surveyed in Section 2 make it possible to look at novel solutions to underwater reception. The extremely low noise levels generated in superconducting circuitry and in SQUID amplifiers make it possible to use a much smaller antenna than the 100 m trailing wire used with conventional receivers. This smaller antenna is poorly matched to the radiation field and collects only a fraction of the available energy. This approach is useful so long as the fraction of noise energy in the environment ($T \geqslant 300$ K) collected by the antenna is larger than the noise temperature of the SQUID. For a dc SQUID amplifier with 20 kHz bandwidth, the equivalent noise temperature is ~0.01 K. For narrower bandwidths it is even smaller. Therefore, the SQUID could be coupled to an antenna that is at least four orders of magnitude smaller than conventional low-frequency antennas.

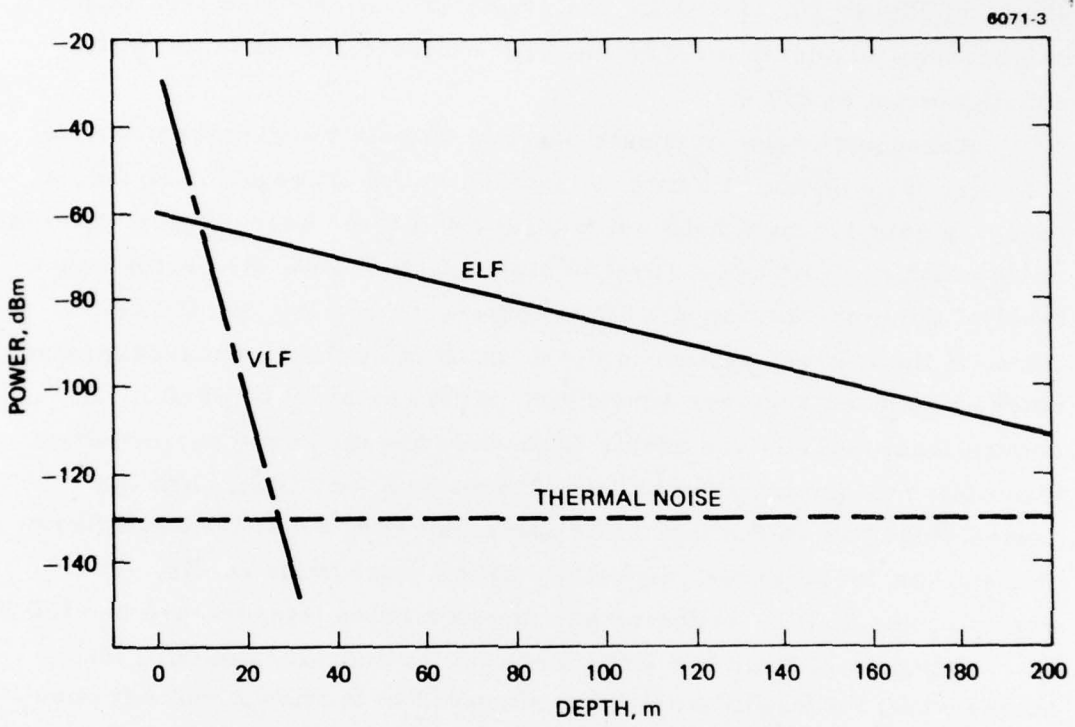

Figure 10. Underwater propagation of ELF and VLF signals. Thermal noise reference is for 300 K and 20 kHz bandwidth.

This basic approach has been followed by NRL in designing a new receiver for submerged ELF communications. The technique should also be applicable to VLF communications, although the potential communication depth is more limited at the higher frequencies.

Another low-frequency application currently being pursued at NCSL is the use of SQUID magnetometers and gradiometers for the localization of magnetic anomalies. These fields have a strong dipole-like characteristic which allows them to be detected independent of the large background magnetic field of the earth. In addition to providing improved sensitivity and detection ranges, it is possible for an array of such sensors to provide greatly improved localization information without the need for extensive motional scanning. Thus, these devices offer substantial improvements for MAD compared to the existing AN/ASW-81.*

B. SIGNAL-PROCESSING APPLICATIONS

Although this study has been very heavily biased toward the application of JEDs in low-noise receivers, it would certainly not be complete without some discussion of the potential impact of these devices upon future signal-processing applications.

System architecture is very strongly influenced by the type of signal processing required to accomplish a given mission. Similarly, the choice of the mission, i.e., the specific requirements for information and data that a system must produce, is limited at times by the signal-processing capabilities available for the job. It would be foolhardy for the system designer to structure his mission so that it required a signal-processing capability beyond the state of the art. Therefore, increasing that level of processing capability should stimulate the designer to structure a system with greater functional capabilities and greater utility. Because of their special properties, JEDs

*A more quantitative discussion of this application can be found in the "Report of the U.S. Navy Nonacoustic ASW Panel," Nov. 1973, prepared by R. N. Keeler, et al., Lawrence Livermore Laboratory, Doc. No. MISC-00973.

offer the possibility of improving the data processing rates and current densities of LSI by an order of magnitude or more. Therefore, their development can have a very significant effect on the design of future systems.

The two most important properties of JEDs, which give them a fundamental advantage over all existing semiconductor logic families, are (1) fast inherent switching speed and (2) low-power operation and small size. Either one of these properties alone would not be enough to give them a substantial advantage over semiconductor circuits. The low-power operation is not useful in power-limited (e.g., battery-run) systems because the power consumed for the cryogenic support system negates any advantage over the low-power semiconductor families. Fast operation alone is not sufficient because GaAs FET and TED logics are capable of comparable speeds for isolated gates and switches. However, when both (1) and (2) above are combined they provide the capability to make high-speed, complex processing circuits with performance that will surpoass the fundamental limits of semiconductor circuits by orders of magnitude.

The low power and small size of the high-speed JEDs means that the circuit elements may be closely packed using cells that may be only several micrometers on a side. By comparison, the high-speed GaAs FET gates must be separated by hundreds of microns in very-large-scale circuits to ensure that heat is removed from the circuit in a simple manner (i.e., assuming parallel heat flow to a plane boundary). This difference could mean that the circuit needed to perform a given complex function would be 100x larger for GaAs FET logic than for JED logic. This size difference would also introduce signal-propagation delays in interconnecting lines that were 10x longer for the GaAs FET circuits.

The similar switching and gate delay times for JEDs and GaAs FETs mean that for relatively simple tasks such as an A/D converter or a frequency divider the two technologies should be able to achieve similar performance (i.e., serial data rates). However, for an integrated signal processor that contains tens of thousands of gates, the

high packing density of the JED technology should yield a significantly faster product. Also, for a high-speed memory, the circuit density is one of the most important parameters. Thus, the JED technology holds great promise for the realization of an integrated, high-speed, compact signal processor that contains A/D circuitry, digital computing capability, and high-density memory, all operating at data rates of 10 Gbit/s or higher.

In addition to the integration of conventional processing architectures in a single, high-speed package, the JED technology will make new system architectures possible. As an example, consider a typical radar where signals are converted from rf to successively lower i.f. frequencies and are amplified until the output frequency and power levels are compatible with the processing circuitry, both analog and digital. With the availability of high-data-rate JED processors, it would probably be possible to eliminate one or two stages of frequency conversion and many stages of amplification because of the low power and noise levels associated with the JEDs. This could result in a much simpler radar with improved performance and reliability.

C. SUMMARY OF MOST IMPORTANT FUTURE APPLICATIONS FOR JEDs

In this section we assign priorities to the potential applications for JEDs. The areas ranked highest are those which we feel need significant development work and those where there is the clearest benefit in terms of improved system performance. Those areas, such as ELF communications and magnetic anomaly detection, where there is great potential benefit but where there is already significant development work underway are not recommended for future phases of this program.

We feel that this study has shown that the greatest impact of JEDs on systems in the near term will come from improvements in receiver sensitivity. This is because the use of an improved receiver does not require any new system design to utilize the new component effectively. For the selected systems discussed in Section 4.A, a

receiver with the capabilities of existing components, but with better sensitivity, can be used to improve the overall system performance. Currently there is insufficient information available about the performance of JEDs and super-Schottky diodes to ensure that this goal can be met. Whichever application is chosen for further exploration, one of the early tasks of the development program should be to identify the specific performance parameters needed and to define the performance of the superconductive devices in those areas.

In comparing the receiver applications discussed in 4.A, the two most promising are the octave bandwidth swept microwave receiver and the millimeter-wave receiver. The tradeoffs for improved sensitivity are not as well established for the microwave receiver as they are for the millimeter-wave application examined. In addition, a component developed for the 94 GHz radar would be readily extendable to the other millimeter-wave applications that are developing. If, however, further study shows that the microwave receiver system could benefit significantly from the improved sensitivity, then the potential near-term benefits would be greater for this application because of the present widespread deployment of this type of system compared to that of millimeter-wave systems.

On the basis of the established need for improved millimeter-wave receiver performance, we feel that the development of this application is most consistent with the goals of the Josephson Junction Technology Program. This development of the 94 GHz receiver is for a ground-based or large-mobile-platform application and could use a simple, dewar-based cryogenic system. Therefore, the utility of the receiver development will not depend on the rapid development of yet another technology, the compact, reliable closed-cycle cooler.

The development program for the millimeter-wave receiver would include mixer device design and development tasks (including trade-off studies on the super-Schottky and JED mixers), mixer circuit design and development tasks, an i.f. amplifier development task, and subsystem integration and testing. The development cycle for this project should last approximately 30 months.

A similar program could be structured for the microwave receiver development except that there would be need for a preliminary study phase to determine the actual system performance benefits to be expected from the receiver development. Typical candidate systems might be the AN/WLR-6 or the AN/WLR-8.

There is one other development option which should be considered for the Josephson Junction Technology Program. Because of the great potential of JEDs for use in high-speed signal processing, the program planners should compare the benefit from a near-term payoff in the receiver technology with the longer term payoff that would result from the development of an integrated high-speed signal-processing capability.

Because the circuits needed for this latter application are much more complex than the receiver circuits the level of development effort needed is much greater. For example a three-year program to develop an A-D converter might be 2-3X the cost of a receiver development, and it would not necessarily produce a component which would be cost effective for use in a system. This is because the cost of introducing cryogenics into the system would not be spread over a significant portion of the system. However, the demonstration of an A-D converter with, for example, a 10 Gbit/s data rate would significantly stimulate ideas for new system designs and give greater importance to the support for the development of the digital processing and memory circuits which would be needed to form an integrated subsystem.

REFERENCES

1. H.H. Zappe, IEEE MAG-13, (1977).
2. R.W. Keyes, Proc. IEEE 63, 740 (1975).
3. Microwaves 15, 9 (Sept., 1976),
4. W. Jutzi Th. O. Mohr, M. Gasser, and H.P. Gschwind, Electronics Lett. 8, 589 (1972).
5. J. Magerlein and T.A. Fulton, Bull. Am. Phys. Soc., March Meeting, 1977, San Diego, California.
6. H.H. Zappe, APL 27, 432 (1975).
7. Millimter Wave Technology Evaluation System, Contract No. F30602-73-C-0191.
8. W. Anacker, IEEE MAG-5, 968 (1969).
9. H.H. Zappe, IEEE SC-10, 12 (1975).
10. R.F. Broom, W. Jutzi and Th. Mohr, IEEE MAG-11, 755 (1975).
11. P. Guéret, APL 25, 426 (1974).
12. H.H. Zappe, APL 25, 424 (1974).
13. P. Guéret, Th. O. Mohr, and P. Wolf, IEEE MAG-13, 52 (1977).
14. W.H. Henkels and H.H. Zappe (To be submitted to IEEE Journal of Solid State Circuits).
15. D.J. Herrell, IEEE SC-10, 360 (1975).
16. D.J. Herrell, IEEE SC-9, 277 (1974).
17. M. Klein, IEEE ISSCC, 202 (1977).
18. R.C. Peterson and D.G. McDonald, IEEE MAG-13, 887 (1977).
19. J. Claassen, Y. Taur and P. Richards, APL 25, 759 (1974).
20. Y. Taur, J. Claassen and P. Richards, APL 24, 101 (1974).
21. M. McColl, M.F. Miller, A.H. Silver, M.F. Bottjer, R.F. Pederson and F.L. Vernon, Jr., IEEE MAG-13, 221 (1977).
22. T. Blaney, Rev. Phys. Appl. 9, 279 (1974).

23. C.L. Huang and T. Van Duzer, IEEE ED-6, 579 (1976).

24. Y. Taur, J.H. Claassen and P.L. Richards, IEEE MTT-22, 1005 (1974).

25. F. Auracher and T. Van Duzer, Proc. 1972, Applied Superconductivity Conf. (Annapolis, Md.) 1972.

26. P.L. Richards, J.H. Claassen, and Y. Taur, Low Temperature Physics – LT-14, M. Krusnio, and M. Vuorio Eds. (American Elsevier, New York, 1975) V. 4.

27. F.L. Vernon, Jr., M.F. Miller, M.F. Bottjer, A.H. Silver, R.J. Pederson, and M. McColl, to be published in IEEE – MTT.

28. H. Kanter and F. Vernon, Jr., JAP 43, 3174 (1972).

29. P. Richards and S. Sterling, APL 14, 394 (1969).

30. H. Tolner, C. Andriesse and H. Schaeffer, Infrared Physics 16, (1976).

31. B. Ulrich, Rev. Phys. Appl. 9, 65 (1974).

32. R.Y. Chiao and P.T. Parish, JAP 47, 2639 (1976).

33. S. Wahlsten, S. Rudner, and T. Claassen, preprint.

34. Y. Taur and P.L. Richards, IEEE MAG-13 252 (1977).

35. A.N. Vystavkin, V.N. Gubanov, L.S. Kuzmin, K.K. Likharev, V.V. Migulin, and V.K. Semenov, IEEE MAG-13, 233 (1977).

36. A.H. Silver, IEEE MAG-11, 794 (1975).

37. P.L. Richards, "Superconducting Quantum Interference Devices and their Applications," H.D. Halbohm and H. Lubbig, Eds. (Walter de Guigter, Berlin-New York, 1977) to be published.

38. T.F. Finnegan and S. Wahlsten, Appl. Phys. Lett. 21, 541 (1972).

39. T.F. Finnegan, J. Toots and J. Wilson, Low Temperature Physics – LT-14, M. Krusnio and M. Vuorio, Eds. (American Elsevier, New York, 1975), V. 4, 184.

40. T.F. Finnegan, private communication.

41. D.W. Jillie, J.E. Lukens, and Y.H. Kao, IEEE MAG-13, 578 (1977).

42. D.W. Palmer and J.E. Mercereau, IEEE Trans. on Magn. MAG-11, 667 (1975).

43. J. E. Lukens, private communication.

44. J. Clarke, W.M. Goubau, and M.B. Ketchen, JLTP 25, 99 (1976).

45. J. Clarke, "Superconducting Quantum Interference Devices and Their Applications," H.D. Hahlbohm and H. Lubbig, Eds. (Walter de Gruyter, Berlin – New York, 1977) to be published.

46. J.M. Pierce, J.E. Opfer, L.H. Rorden, IEEE MAG-10, 599 (1974).

47. L.D. Jackel and R.A. Buhrman, JLTD 19, 201 (1975).

48. J.R. Davis and M. Nisenoff, preprint.

49. W.S. Goree, Proc. Applied Superconductivity Conference (Annapolis) 1972.

50. W. Wynn, C. Frahm, P. Carroll, R. Clark, J. Wellhoner, and M. Wynn, IEEE MAG-11, 701 (1975).

51. M.B. Ketchen, W.M. Goubau, J. Clarke, and G.B. Donaldson, IEEE MAG-13, 372 (1977).

52. R.P. Giffard, R.A. Webb, and J.C. Wheatley, JLTP 6, 533 (1972).

53. Y. Taur, J. Claassen and P. Richards, Rev. Phys. Appl. 9, 263 (1974).

54. R. S. Avakjan, A. N. Vystavkin, V.N. Gubankov, V. V. Migulen and V. D. Shtykov, IEEE MAG-11, 838 (1975).

55. S. Weinrieb and A. Kerr, IEEE MTT 23, 781 (1975).

56. H. Fetterman, B. Clifton, P. Tannenwald, C. Parker and R. Penfield MTT 22, 1013 (1974).

57. H. L. St over, H. M. Leedy, and R. P. Bryan, 1973 IEEE International Sol. St. Circuits Conf. Digest of Tech. Papers, p. 80.

58. J. Clark, G. Hoffer, P. Richards, Rev. Phys. Appl. 9, 69 (1974).

59. J. Clark and T. Hsian, IEEE MAG 11, 845 (1975).

60. J. Clark, G. Hoffer, P. Richards and N. Yek, Int. Conf. on Low Temp. Phys. LT 14 Finland, 226 (1975).

61. N. Coron, G. Dambier, J. Leblanc and J. Moalic, RSI 46, 492 (1975).

62. M. McColl, M. Miller and A. Silver, APL 23, 263 (1973).

63. M. J. Feldman, P. T. Parrish and R. Y. Chiao, JAP 46, 4031 (1975).

64. H. Kanter, IEEE MAG-11 789 (1975).

65. M. R. Gaerttner, to Int. Mag. Cont., Toronto (1974).

66. J. Clark, Proc. IEEE 61, 8 (1973).

67. R. Adair, M. Simmonds, R. Kamper and C. Hoer, IEEE IM-23, 375 (1974).